Electronic Supplementary Information - Low-carbon transition pathways of power systems for Guangdong-Hongkong-Macau Region in China

Zuming Liu[a,*], Mingquan Li[b], Edgar Virguez[c], Xiaomin Xie[d,e,*]

[a]College of Smart Energy, Shanghai Jiao Tong University, Shanghai, 200240, China
[b]School of Economics and Management, Beihang University, Beijing, 100191, China
[c]Department of Global Ecology, Carnegie Institution for Science, Stanford University, California, United States
[d]Research Institute of Carbon Neutrality, Shanghai Jiao Tong University, Shanghai, 200030, China
[e]School of Mechanical Engineering, Shanghai Jiao Tong University, Shanghai, 200240, China

Summary

This supplementary provides detailed information for studying transition pathways of power systems for Guangdong-Hongkong-Macau (GHM) region in China. Section S1 presents existing capacities of generation, storage, and transmission infrastructure, as well as electricity load projection for GHM region. Section S2 elaborates methodologies for evaluating renewable energy resources, including solar, wind, and biomass. Section S3 details model formulation and solution strategy for studying transition pathways of GHM power system. Sections S4 and S5 provide model input data and design potential decarboniation scenarios for GHM power system. The supplemental figures from decarbonization analyses are presented in Section S6.

Contents

*Corresponding author. E-mail: zmliu@sjtu.edu.cn, xiexiaomin@sjtu.edu.cn.

S1 Energy infrastructure and electricity loads

S1.1 Existing fossil fuel generation

The information of fossil fuel generation including coal- and gas-fired plants is obtained from Global Coal Plant Tracker[1] and Energy Bureau of Guangdong Province[2]. The Global Coal Plant Tracker provides detailed information for global coal-fired generation, such as plant name, location, capacity, status, combustion technology, remaining lifetime, etc. For gas-fired generation, we use the data provided by Energy Bureau of Guangdong Province, which lists important information of gas-fired generation in Guangdong province, including plant name, location, capacity, number of units, commissioning year, and lifetime. Here, we consider fossil fuel generation that has been operating or under construction in Guangdong-Hongkong-Macau (GHM) region. There are a total number of 148 coal-fired units and 89 gas-fired units in GHM region, and their geographical distributions are shown in Figure S1, from which we can see that most of coal- and gas-fired units are deployed in Pearl River Delta Region due to its prosperous economic activities. Only a few coal- and gas-fired plants are deployed in eastern, western, and northern Guangdong province. The overall capacities of existing coal- and gas-fired generation in Guangdong province are 65,121 MW and 28,237 MW, which agrees well with those (64,270 MW and 28,380 MW) reported by the 14th Five-Year Energy Development Plan of Guangdong Province[3]. Moreover, coal- and gas-fired generation in both Hongkong and Macau reaches 6108 MW and 3525 MW, respectively. The economic parameters and operating characteristics of coal- and gas-fired generation technologies are presented in Section S4.

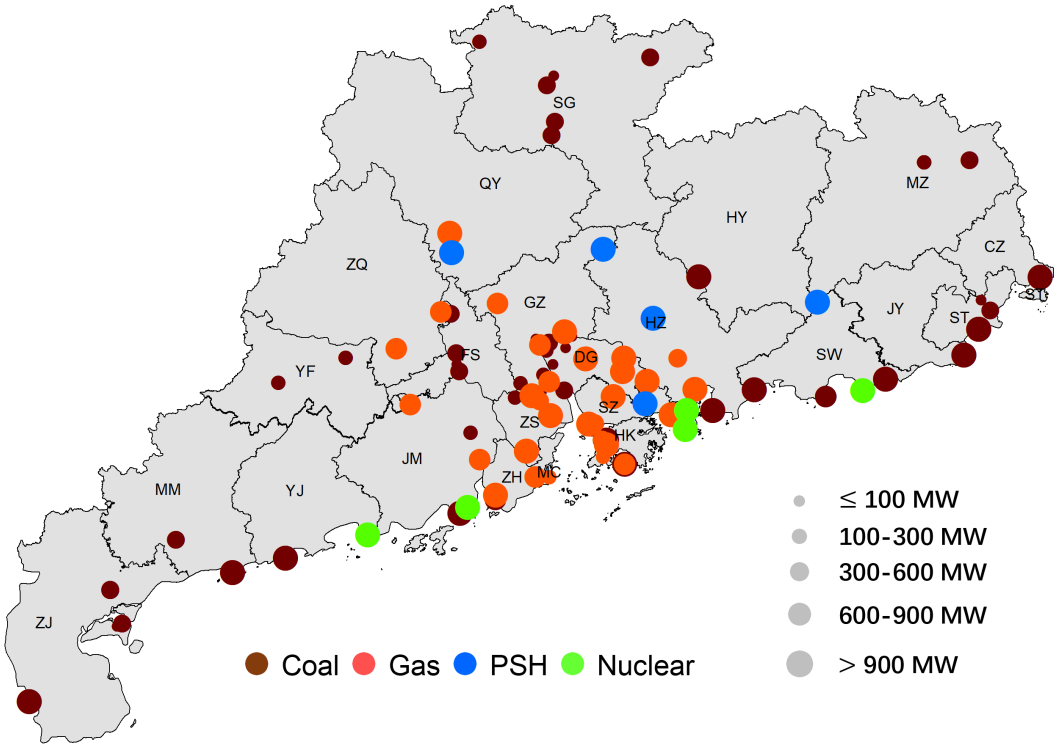

Figure S1 Geographical distribution of existing fossil fuel and nuclear generation as well as pumped storage hydropower generation in GHM region.

Table S1 Existing solar and wind generation capacities in GHM region. NA means offshore wind installation is not applicable for inland cities.[4–6]

City	Solar PV [MW]	Onshore wind [MW]	Offshore wind [MW]
Guangzhou	700	-	NA
Shenzhen	1,190	-	NA
Zhuhai	300	63	420
Shantou	600	333	950
Foshan	700	-	NA
Shaoguan	890	317	NA
Heyuan	450	347	NA
Meizhou	800	100	NA
Huizhou	500	149	400
Shanwei	220	310	500
Dongguan	390	-	NA
Zhongshan	206	-	NA
Jiangmen	600	251	-
Yangjiang	180	458	1,700
Zhanjiang	1,406	1,258	400
Maoming	348	402	-
Zhaoqing	208	150	NA
Qingyuan	880	693	NA
Chaozhou	100	137	NA
Jieyang	26	260	900
Yunfu	130	78	NA

Table S2 Existing nuclear power plants in GHM region.

Name	Citiy	Number of units	Capacity [MW]
Yangjiang Nuclear Power Plant	Yangjiang	5×1,080 MW	5,400
Ling'ao Nuclear Power Plant	Shenzhen	2×990 MW, 2×1,080 MW	4,140
Taishan Nuclear Power Plant	Jiangmen	2×1,750 MW	3,500
Daya Bay Nuclear Power Plant	Shenzhen	2×900 MW	1,800
Lufeng Nuclear Power Plant	Shanwei	2×1,000 MW	2,000

Table S3 Existing pumped storage hydropower stations in GHM region.

Name	City	Number of units	Capacity [MW]
Huizhou Pumped Storage Power Station	Huizhou	8×300 MW	2,400
Guangzhou Pumped Storage Power Station	Guangzhou	8×300 MW	2,400
Meizhou Pumped-storage Hydro Power Station	Meizhou	8×300 MW	2,400
Qingyuan Pumped Storage Power Station	Qingyuan	4×320 MW	1,280
Shenzhen Pumped Storage Power Station	Shenzhen	4×300 MW	1,200

S1.2 Existing clean energy generation

The clean energy generation considered in this work is composed of solar, wind, nuclear, hydro, and biomass generation technologies. The existing capacities of solar and wind generation are obtained from Energy Bureau of Guangdong Province, which provides detailed development plans of solar, onshore wind, and offshore wind generation[4–6]. Table S1 shows the installed capacities of solar and wind generation in GHM region. The hourly capacity factors of solar and wind are obtained using meteorological dataset from NASA data center[7]. The dataset provides hourly solar irradiance, wind speed, and temperature from 2001-2018 for locations all over the world. A geographical information system analysis is performed to obtain hourly solar and wind capacity factors for each city in GHM region. The hourly generation of existing solar and wind facilities can be determined by mapping hourly capacity factors to their installed capacities. More details on obtaining hourly solar and wind capacity factors can be found in Section S2.

Nuclear and hydro generation is of great importance to GHM region. Five nuclear power plants have been deployed in Guangdong, with an overall capacity of 16,840 MW[3]. Their names, located cities, number of units, as well as capacities are shown in Table S2. Hydro generation comprises generation from pumped storage hydropower (PSH) stations and hydropower plants. Five large-scale PSH stations have been built in Huizhou, Guangzhou, Meizhou, Qingyuan, and Shenzhen, with an overall capacity of 9,680 MW as can be seen in Table S3[2]. The geographical distribution of nuclear and PSH plants are presented in Figure S1. Beside PHS stations, reservoir hydropower plants are deployed in eastern, western, and northern Guangdong[8]. The installed capacity of reservoir hydropower plants in each city is shown in Table S4, and their total capacity reaches 7,620 MW[9]. It is worth mentioning that Shenzhen (SZ), Zhuhai (ZH), Shantou (ST), Foshan (FS), Dongguan (DG), and Zhongshan (ZS) hold very small hydropower capacities, while there is no hydropower generation in Hongkong (HK) and Macau (MC). Hence, these cities are not presented in Table S4.

Biomass energy is now receiving growing attention in GHM region. The total installed capacity of

biomass generation reaches 2800 MW in 2020, of which agricultural and forestry biomass generation as well as urban waste generation account for 45% and 52%, respectively[10]. It is difficult to find the installed capacity of biomass plants in each city from open literature. For this, we distribute the total waste generation capacity to each city according to their current waste processing capacities[11]. Moreover, we allocate the total generation capacity of agricultural and forestry biomass to each city according to their abundance as shown in Figure S7. As such, we can obtain the installed biomass generation capacity for each city in GHM region as presented in Table S5. The economic parameters and operating characteristics of clean energy generation technologies are detailed in Section S4.

Table S4 Existing hydropower capacity in GHM region.

City	Abbreviation	Capacity [MW]	City	Abbreviation	Capacity [MW]
Guangzhou	GZ	130	Zhanjiang	ZJ	64
Shaoguan	SG	1,633	Maoming	MM	442
Heyuan	HY	637	Zhaoqing	ZQ	555
Meizhou	MZ	1,274	Qingyuan	QY	1,157
Huizhou	HZ	251	Chaozhou	CZ	159
Shanwei	SW	113	Jieyang	JY	273
Jiangmen	JM	196	Yunfu	YF	349
Yangjiang	YJ	387	-	-	-

Table S5 Existing biomass generation capacity in GHM region.

City	Abbreviation	Capacity [MW]	City	Abbreviation	Capacity [MW]
Guangzhou	GZ	252	Jiangmen	JM	89
Shenzhen	SZ	244	Yangjiang	YJ	48
Zhuhai	ZH	42	Zhanjiang	ZJ	258
Shantou	ST	125	Maoming	MM	199
Foshan	FS	163	Zhaoqing	ZQ	172
Shaoguan	SG	111	Qingyuan	QY	111
Heyuan	HY	75	Chaozhou	CZ	57
Meizhou	MZ	111	Jieyang	JY	76
Huizhou	HZ	180	Yunfu	YF	48
Shanwei	SW	68	Hongkong	HK	47
Dongguan	DG	191	Macau	MC	31
Zhongshan	ZS	103	-	-	-

S1.3 Existing transmission networks

The existing inter-city transmission lines are adopted from China Southern Power Grid Operation Manners[12]. This operation guideline lists detailed network topology of transmission lines among cities. There are more than 200 500 kV AC transmission lines and 60 500 kV transformation stations in GHM region. Including all of them into model formulation will be very challenging and incurs the optimization problem numerically intractable. Here, to reduce network complexity, we merge all transformation stations in each city into a node, and use a merged transmission line to represent

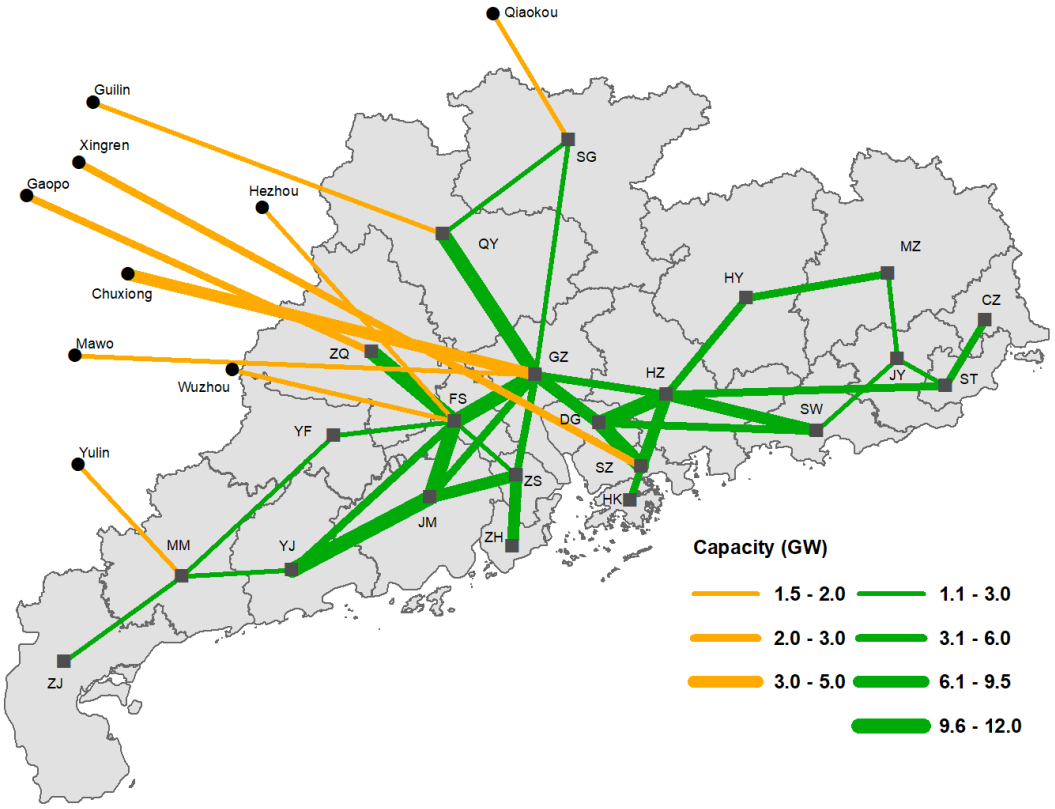

Figure S2 Existing power transmission networks for west-east power transmission and inter-city power transmission in GHM region. The data are obtained from China Southern Power Grid Operation Manners.[12] The brown lines are transmission lines for importing electricity from cites other provinces, while the green lines represent 500 kV AC transmission lines for inter-city power transmission.

power transmission corridor between cities, as shown in Figure S2. The transmission network extends from its center cities (Guangzhou, Foshan, and Dongguan) to western, northern, and eastern GHM region. The existing inter-city transmission lines and their respective capacities are presented in Table S6. Moreover, to meet the power deficit in GHM region, nine inter-province transmission lines, connecting cities in Guangxi, Guizhou, Yunnan, and Hunan provinces, have been built for west-to-east power transmission. The capacities of these inter-provincial transmission lines range from 1500 MW to 5000 MW as shown in Table S7[13].

S1.4 Load profiles and prediction

Electricity load is coupled with a number of socio-economic factors, which makes its accurate prediction very challenging. A few studies assume constant growth rates in different periods for electricity load projection[14,15], while others employ computable general equilibrium (CGE) models that consider population, economy, and policies for electricity demand prediction[16]. CGE models require extensive input data, including detailed information on consumer behaviors, economic variables, and energy polices. Obtaining accurate and comprehensive data can be challenging, leading to inaccuracies in predictions of electricity demand, especially in long-term predictions. Having this in mind, we employ autoregressive moving average (ARMA) model, a time-series analysis method, for future electricity load prediction. This time-series analysis method was found to be capable of providing satisfactory predictions[17].

Table S6 Existing transmission lines among cities in GHM region.[12]

Transmission line -	Distance [km]	Capacity [GW]	Transmission line -	Distance [km]	Capacity [GW]
Qingyuan-Guangzhou	128	9.815	Heyuan-Huizhou	101	3.62
Qingyuan-Shaoguan	107	1.415	Guangzhou-Dongguan	56	9.2
Shaoguan-guangzhou	166	2.83	Shanwei-Huizhou	108	8.415
Maoming-Yangjiang	86	3.0	Jiangmen-Zhongshan	80	8.0
Maoming-Yufu	125	2.411	Zhuhai-Zhongshan	41	7.24
Zhanjiang-Maoming	132	2.0	Chaozhou-Shantou	54	3.62
Guangzhou-Huizhou	100	4.63	Meizhou-Jieyang	96	2.83
Huizhou-Shenzhen	75	9.18	Meizhou-Heyuan	116	3.54
Huizhou-Dongguan	73	10.517	Shantou-Huizhou	215	3.99
Fushan-Guangzhou	71	10.476	Jieyang-Shanwei	71	2.83
Yangjiang-Foshan	162	3.99	Shantou-Jieyang	49	2.83
Yangjinag-Jiangmen	97	11.882	Guangzhou-Zhongshan	90	3.99
Foshan-Zhaoqing	96	11.76	Zhongshan-Foshan	71	2.83
Jiangmen-Foshan	86	10.643	Shanwei-Dongguan	171	3.99
Guangzhou-Jiangmen	147	3.99	Foshan-Yunfu	121	1.114
Dongguan-Shenzhen	42	10.44	Shenzhen-Hongkong	30	3.6

Table S7 Existing transmission lines for importing electricity to GHM region.[13]

Transmission line -	Distance [km]	Capacity [GW]	Transmission line -	Distance [km]	Capacity [GW]
Qiaokou-Shaoguan	135	2.0	Chuxiong-Guangzhou	1237	5.0
Guilin-Qingyuan	282	1.5	Mawo-Guangzhou	263	1.8
Hezhou-Foushan	209	1.5	Wuzhou-Foshan	179	1.6
Xingren-Shenzhen	963	3.0	Yulin-Maoming	107	2.1
Gaopo-Zhaoqing	625	3.0	-	-	-

The future load profile of each city is derived by load predictions via ARMA model using historical load data between 2001 and 2020 from Guangdong Statistical Yearbook[18], Hongkong Census and Statistical Department[19], and Macau Statistical Yearbook[20]. Historical electricity load can be considered as a representation of GHM socio-economic developments. The load data are used to train ARMA model for predicting electricity loads from 2021 to 2050. The ARMA model is specified with two parameters as follows:

$$ARMA\,(p,q) = c + \sum_{i=1}^{p} \phi_i y_{t-i} + \varepsilon_t + \sum_{j=1}^{q} \theta_j \varepsilon_{t-j} \tag{S1}$$

where c, ϕ_i and θ_j are coefficients, p is the lag order, q is the order of the moving average, and ε_t is an error term that follows Gaussian distribution. The values of p and q and coefficients can be determined using historical load data between 2001 and 2020 in MATLAB Econometrics Toolbox[21]. The historical loads and predicted loads agree well as shown in Figure S3, indicating that ARMA model is capable of load prediction. The electricity loads of each city from 2021 to 2050 predicted by ARMA model are shown in Figure S4.

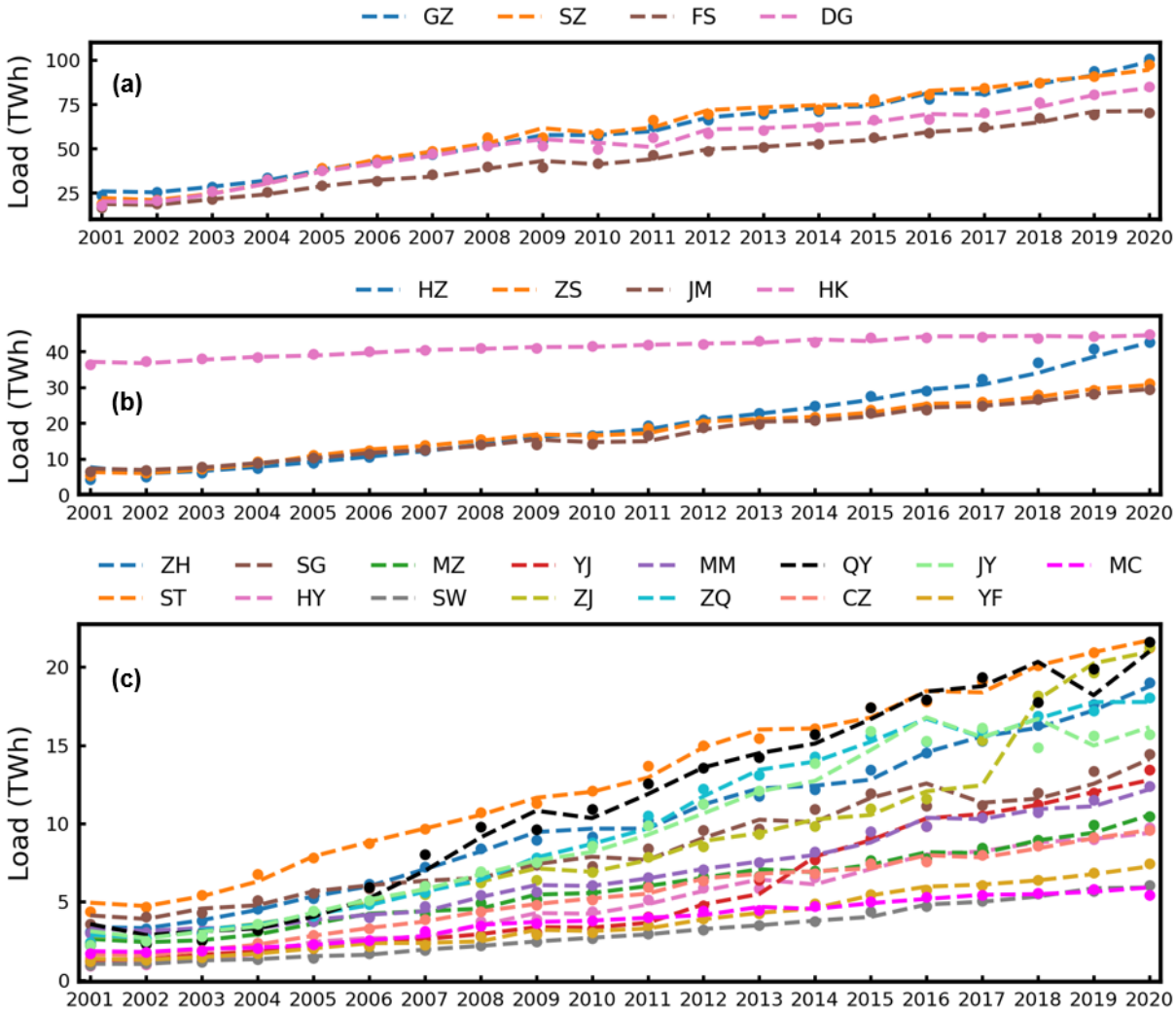

Figure S3 Load profiles of each city in GHM region from 2001 to 2020: (a) high-load cities, (b) medium-load cities, and (c) low-load cities.
Dot represents historical electricity load, while dashed line represents model predictions.

From Figures S3-S4, we can see that cities in GHM region can be classified into three categories (high-load, medium-load, and low-load cities) according to their electricity loads. Guangzhou, Shenzhen, Foshan, and Dongguan are high-load cities, and the electricity loads of Guangzhou and Shenzhen are higher than 100 TWh in 2020 and 200 TWh in 2050. Huizhou, Zongshan, Jiangmen, and Hongkong are medium-load cities; their electricity loads range from 40 TWh to 88 TWh through 2050. Other cities are low-load cities and their loads are lower than 50 TWh in 2050.

The hourly load profiles of each city are needed for studying power system transition in GHM region. For this, we choose three representative cities (Guangzhou, Huizhou, and Shantou) to represent high-load, medium-load, and low-load cities, respectively, and use their demand curves in four typical days (spring, summer, autumn, and winter) in 2020 as shown in Figure S5 for load scaling. The spring, summer, autumn, and winter seasons assume 92, 92, 91, and 90 days to account for their respective duration in a year. The hourly load profile of a city from 2021 to 2050 is obtained by scaling up/down its representative city's hourly load profile in 2020 using its annual loads as shown in Figure S4. As such, we can determine the future hourly load profiles of every city in GHM region from 2021 to 2050.

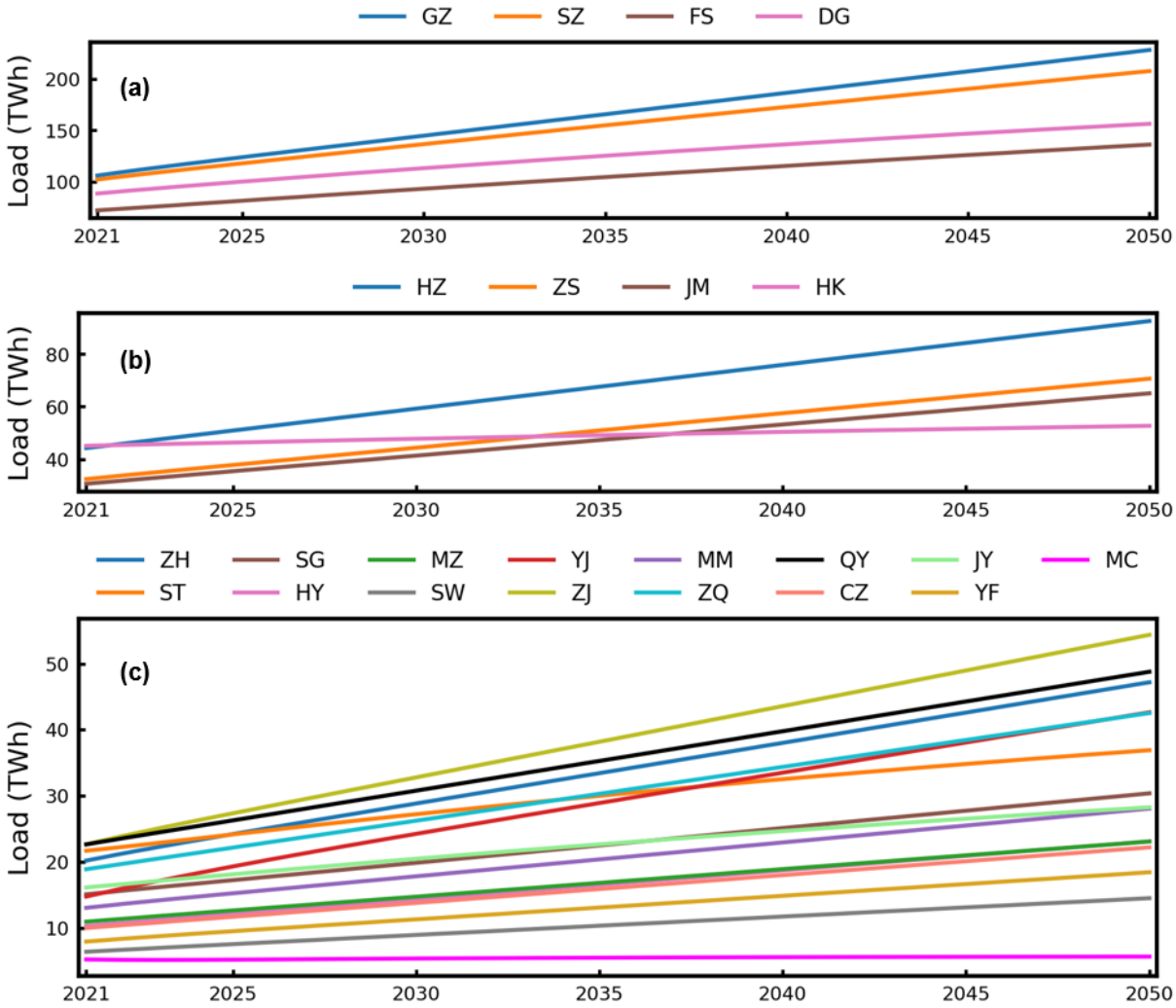

Figure S4 Load profiles of each city in GHM region from 2021 to 2050 through prediction: (a) high-load cities, (b) medium-load cities, and (c) low-load cities.

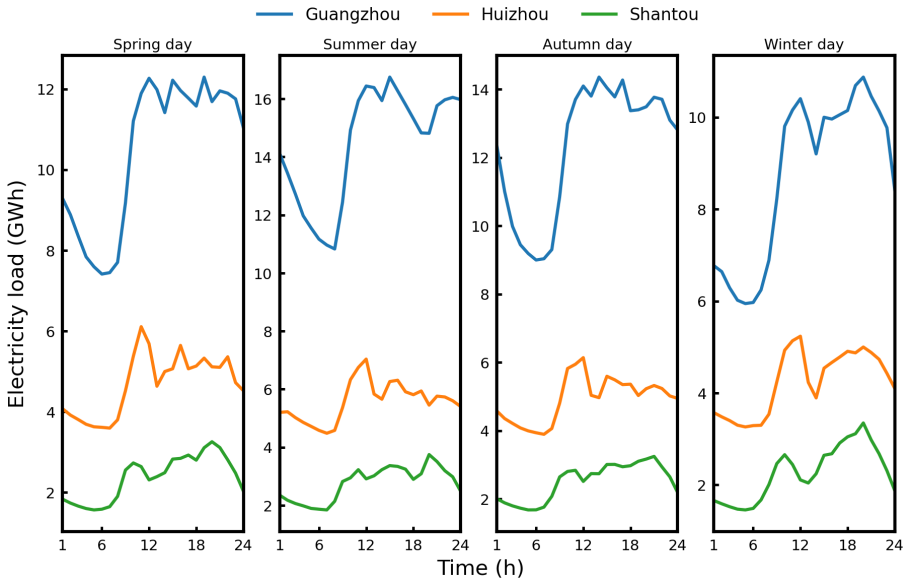

Figure S5 Electricity loads of Guangzhou, Huizhou, and Shantou in spring, summer, autumn, and winter days in 2020.

S2 Renewable energy evaluation

The non-hydro renewable energy we consider in this work are solar, wind, and biomass energies. Their potential capacities and capacity factors are needed for energy system planning. The procedure for determining solar and wind potential capacities and their capacity factors follows Li et al.'s method[22] and comprises four steps: (1) determine hourly wind and solar capacity factors from wind speed and solar irradiance in each grid cell of GHM region. The obtained capacity factors are employed to select grid cells that satisfy minimum deployment requirements. (2) perform a geographical information system (GIS) analysis based on selected grid cells using land use data[23], surface elevation and slope information[24], and geomorphology[25] to assess suitable site areas in each cell for deploying solar PV and wind turbines. (3) estimate maximum installation capacity of each suitable site, and obtain potential capacity of power generation for each city by aggregating capacity of each suitable site within its boundary. (4) average hourly capacity factors of all suitable sites in each city and determine hourly solar and wind power generation from their installed capacities for each city.

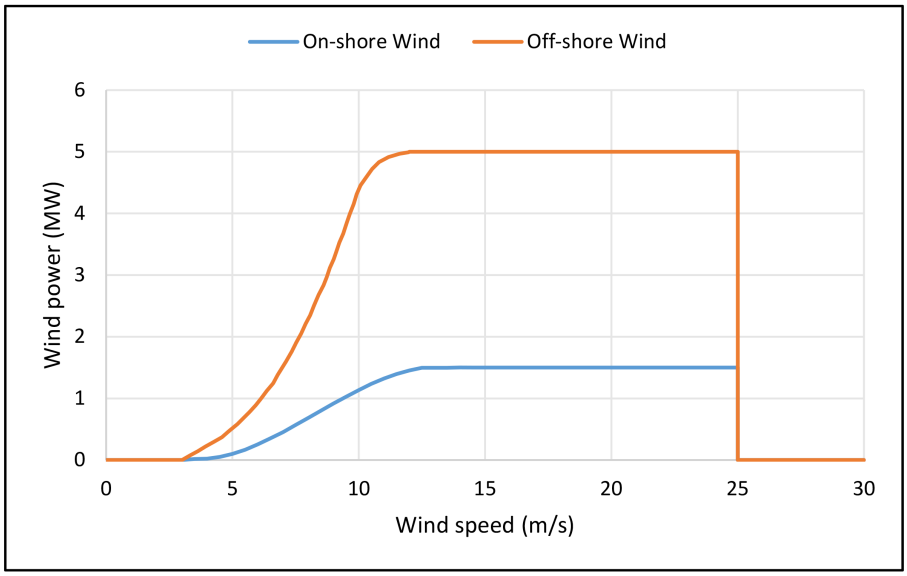

Figure S6 Power curves of onshore and offshore wind turbines for hourly capacity factor evaluation in GHM region.

S2.1 Onshore wind

The hourly wind capacity factor is determined using historical wind speed data from NASA's MERRA-2 dataset[7] and power curve of a 1.5 MW General Electric (GE) wind turbine. The MERRA-2 dataset provides hourly meteorological data from 2000-2018 for each of 0.5°×0.625° grid cell in China. The wind speed from MERRA-2 dataset is measured at 50 meter's height. The power curve of GE wind turbine, as shown in Figure S6, is characterized by three wind speeds: cut-in speed (v_{ci} = 3.5 m/s), rated speed (v_r = 14.5 m/s), and cut-out speed (v_{co} = 25 m/s). We assume wind turbines deployed in GHM region have a hub height of 100 meter. The wind speed (v_{hub}) at the hub height (h_u)

can be determined using the wind speed (v_{mea}) at the measured height (h_0) via power law as follows:

$$v_{hub} = v_{mea}\left(\frac{h_u}{h_0}\right)^{0.143} \tag{S2}$$

The hourly wind capacity factor for each grid cell is then obtained by looking up the power curve of GE wind turbine using hub height wind speed. The grid cells with an annual capacity factor of less than a threshold value should be excluded. Other criterion for area exclusion are set by land use data[23], surface elevation information[24], and geomorphology[25]. The land use data, with a spatial resolution of 1,000 m × 1,000 m geographical grid, comprises 6 primary land types and 25 secondary land types. The surface elevation and slope information is obtained from digital elevation model (DEM), which provides elevation of each geographical grid (90 m × 90 m) and slope between adjacent grids. The geomorphology data features a spatial resolution of 1:1,000,000 and provides various landform types of plains, platforms, hills, and mountains. The above information can be used to determine suitable geographic grids, also called sites here, for onshore wind installation. The detailed parameter setting for identifying suitable sites for onshore wind turbines can be found in Li et al.[22] After identifying suitable sites of 90 m × 90 m for onshore wind installation, we determine each site's maximum installation capacity by assuming a capacity density of 8 W/m^2 [26]. We then obtain the potential capacity of onshore wind generation for a city by aggregating the maximum installation capacity of each suitable site within its administrative boundary. The hourly wind power generation in a city is computed by multiplying its installed capacity with its hourly capacity factor averaged from all its suitable sites.

S2.2 Offshore wind

Here, we assume offshore wind turbines can be deployed within the exclusive economic zones (EEZ)[27] under the administrative jurisdiction of GHM region. The grid cells suitable for deploying offshore wind turbines are identified using General Bathymetric Chart of the Oceans[28], which provides gridded bathymetric data with 15 arc-second spatial resolution. Zeyringer et al.[29] concluded in their work that a depth of 70 meters is technically feasible for offshore wind. We adopt this assumption here and screen out grid cells with an ocean depth of deeper than 70 meters. Moreover, a distance of 10 km away from coastlines is added for buffer areas. The remaining offshore grid cells are attributed to coastal cities based on minimum Euclidean distance between grid centroids and city coastlines. The wind speed data and processing procedure for offshore wind are the same as onshore wind. A GE offshore wind turbine, with cut-in, rated, and cut-out speed of 3.5, 12, and 25 m/s as shown in Figure S6, is employed to compute hourly capacity factor, while a capacity density of 15 W/m^2 [26] is assumed to determine offshore wind potential capacity for coastal cities.

S2.3 Solar PV

The hourly solar irradiance taken from NASA's MERRA-2 dataset is used to determine solar PV capacity factor. However, the solar irradiance is overestimated due to the imperfect parameterizations and errors on clouds and aerosols. A calibration approach proposed by Feng et al.[30] is adopted here

to adjust the data before computing PV capacity factor. The calibrated solar irradiance is then fed into NREL PWatts[31] to obtain hourly PV capacity factor. The suitable sites for PV installation in each city are identified using land use data[23], surface elevation information[24], and geomorphology[25]. The processing procedure is similar to onshore wind turbines. More details on parameter setting for filtering suitable sites for PV installation can be referred to Li et al.'s method[22]. The maximum installation capacity of each site is derived by assuming a capacity density of 50 W/m^2 [22], after identifying all suitable sites of 90 m × 90 m for PV installation. The PV potential capacity for each city is then obtained by aggregating maximum installation capacity of each suitable site within its administrative boundary. Finally, hourly PV generation is determined by mapping hourly averaged capacity factor to installed capacity in each city.

S2.4 Biomass

The biomass considered in this work comprises agricultural biomass, forestry biomass, and urban waste. Agricultural biomass consists of residues of rice and sugarcane, as they account for more than 99% of food and economic crops in GHM region. Forestry biomass is composed of residues from wood logging, processing, and lumbering, fuelwood processing, bamboo processing as well as urban greening. The data for assessing these biomass potentials can be found in Guangdong Statistical Yearbook[18] and Guangdong Statistical Yearbook on Agriculture[8]. The two yearbooks provide detailed information on agriculture, forestry, and urbanization of each city in GHM region. Rice residues comprise rice straw and husk, while sugarcane residues are composed of bagasse and leaves. The agricultural biomass potential is assessed as follows:[32]

$$\begin{aligned} E_{agbio} = &(1-\delta_{rice})\left(\alpha_{str}LHV_{str}+\beta_{hus}LHV_{hus}\right)Yd_{rice} \\ &+(1-\delta_{sugn})(\alpha_{bag}LHV_{bag}+\beta_{lea}LHV_{lea})Yd_{sugn} \end{aligned} \tag{S3}$$

where α (β) is the ratio of straw or bagasse (husk or leaves) to crop annual productivity, δ is the water content of residue, Yd is the crop annual productivity, and LHV is the lower heating value.

The residues from wood logging (Lc), lumbering (Lb), and processing (Lh), fuelwood processing (Fw), and bamboo processing (Bh) can be determined as follows:[33]

$$\begin{cases} Lc = a_w \frac{o_c}{o_t} Pl + \frac{f_c}{100} dP_e A_e \\ Lb = a_w \frac{100-o_c}{o_t}\left(Pl + \frac{f_c}{100} dP_{el} A_e\right) \\ Lh = a_w \frac{c_h}{100}\left(Lf + \frac{f_c}{100}\frac{c_e}{100} dP_{el} A_e\right) \\ Fw = a_w F_v \\ Bh = w_b \frac{c_p}{100} Bl \end{cases} \tag{S4}$$

where A_e is the area of economic forests, Pl is the crude wood productivity, Lf is the amount of wood for lumbering, Fv is the fuelwood productivity, and Bl is the bamboo productivity. These data can be found in Guangdong Statistical Yearbook on Agriculture[18]. The values of other parameters in Eq. (S4) are obtained from open literature[33]. Moreover, lots of forestry residues are produced from

urban greening. For example, Shenzhen produced 379,000 ton urban greening residues in 2015[34]. The urban greening residues are proportional to the areas of urban parks and green spaces (A_{green}) and thus can be computed using a conversion factor (c_g) as follows:

$$Bu = c_g A_{green} \tag{S5}$$

The forestry biomass potential is determined using low heating values (LHV_{fore} and LHV_{green}) of forestry residues as follows:

$$\begin{aligned} E_{forbio} =& (1-\delta_{fore})\,(Lc + Lb + Lh + Fw + Bh)\,LHV_{fore} \\ &+ (1-\delta_{fore}) BuLHV_{green} \end{aligned} \tag{S6}$$

Urban waste is also an important biomass resource and its energy potential can be determined as follows:

$$E_{uw} = (1-\delta_w)\,c_w U_w LHV_w \tag{S7}$$

where c_w is a conversion factor, U_w is the yield of urban waste, and LHV_w is the waste lower heating value. The Guangdong Statistical Yearbook provides only provincial urban waste yield[18]; however, it can be distributed to every city based on city population. The total biomass energy potential is obtained by summing up potentials of agricultural biomass, forestry biomass, and urban waste.

The geographical distribution of biomass potential in GHM region is shown in Figure S7. Cities in western Guangdong are rich in agricultural and forestry biomass potential, while cities such as Guangzhou, Shenzhen, and Hongkong feature high urban waste potential. The energy potentials of agricultural biomass, forestry biomass, and urban waste reach 53,385, 45,512, and 24,450 GWh, respectively, totaling 123.3 TWh. The biomass potential in GHM region is relatively small, as its annual maximum generation reaches only 34.5 TWh, considering a conversion efficiency of 0.28 as shown in Table S11. This only accounts for 4.67% of GHM annual demand in 2021.

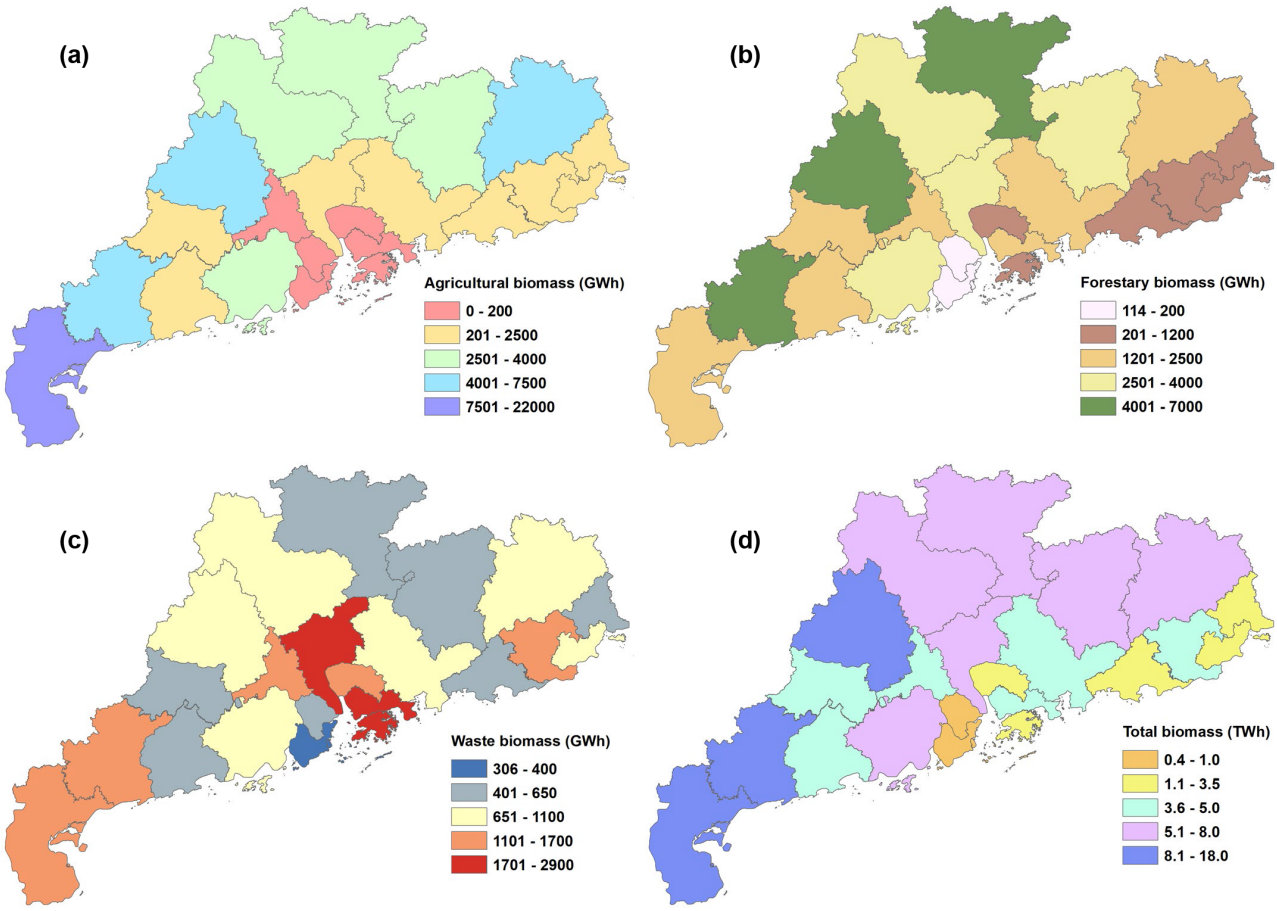

Figure S7 Biomass potential of each city in GHM region, including agricultural and forestry biomass and urban waste.

The GHM region's total biomass potential reaches 123.3 TWh, of which agricultural biomass, forestry biomass, and urban waste account for 53,385 , 45,512, and 24,450 GWh, respectively.

S3 Model formulation for GHM power system

Here, we consider a set of potential generation and storage technologies for low-carbon transition of GHM power system. Generation technologies comprise clean energy technologies and fossil-based technologies. Clean energy technologies consist of solar photovoltaics (PV), onshore wind turbines, offshore wind turbines, biomass, hydro, and nuclear, while fossil-based generation technologies are composed of combined cycle gas turbine (CCGT), combined cycle gas turbine with carbon capture and storage (CCGT-CCS), coal-fired generation (Coal), and coal-fired generation with carbon capture and storage (Coal-CCS). Moreover, pumped storage hydropower (PSH) and lithium-ion battery (LiB) are included as energy storage technologies for system planning. Biomass energy with carbon capture and storage is a negative carbon emission technology; however, we do not consider this technology here due to GHM's relatively small biomass potential, as shown in Section S2.4.

The following assumptions are adopted during model building process for planning GHM power system transition:

- The power system is designed from a perspective of monopolistic planner.
- The electricity demand and electricity import prices are assumed to be inelastic.

- Energy losses during power transmission are a linear function of power flow and transmission distance.
- There are no uncertainties in model parameters, and technology cost learning is assumed exogenously to reduce computation burden.
- The planning horizon is 30 years from 2021 to 2050 with 2021 as initial year, and investment decisions for generation, storage, and transmission capacities are made every 5 years.

For clear and precise clarification, we define the following sets before presenting model formulation for low-carbon power system transition. Moreover, we provide a detailed description of symbols used for model formulation in Section S3.1.

- Years in a given planning horizon: $YM = \{y \mid 1, 2, \cdots, Y\}$;
- Hours in a year: $HM = \{h \mid 1, 2, 3, \cdots, H\} = \{h \mid 1 + 24\,(d-1), \cdots, 24d,\ d = 1, 2, 3, \cdots\}$, where $H = 24 \max[d]$ and d represents design day of type d in a year.
- Generation technologies: $g \in G$, storage technologies: $s \in S$, transmission lines: $m \in M$ and $mx \in MX$, and cities in a given region: $z, \bar{z} \in Z$;
- Useful operation years of technology (generation and storage) e ($e = g \cup s$) installed in city z year n ($n = 0, 1, 2, \cdots$) during a given planning horizon:

$$J_{e,z,n} = \begin{cases} (e, z, n, y)\,|_{n=0} & y \geq 1, y \leq \min[L_{e,z}, Y] \\ (e, z, n, y)\,|_{n\geq 1} & y \geq n, y \leq \min[N_e + n - 1, Y] \end{cases} \tag{S8}$$

  where $n = 0$ denotes the installation year of existing technologies, $L_{e,z}$ is the remaining lifetime of existing technology e in city z, and N_e is the lifetime of new technology e. Here, an existing technology e comprises all of its existing units u and is represented by aggregating all of its existing units. Hence, $L_{e,z}$ equals the maximum remaining lifetime of its existing units u, namely $L_{e,z} = \max\left[L^u_{e,z}\right]$. The capacity of existing technology e over $L_{e,z}$ should be determined by aggregating the capacities of its existing units u over their respective remaining lifetime.
- Useful operation years of transmission line m connecting cities z and $\bar{z}$ installed in year n during a given planning horizon:

$$J_{m,z,\bar{z},n} = \begin{cases} (m, z, \bar{z}, n, y)\,|_{n=0, z<\bar{z}} & y \geq 1, y \leq \min[L_{m,z,\bar{z}}, Y] \\ (m, z, \bar{z}, n, y)\,|_{n\geq 1, z<\bar{z}} & y \geq n, y \leq \min[N_m + n - 1, Y] \end{cases} \tag{S9}$$

  where $n = 0$ denotes the installation year of existing transmission lines, $L_{m,z,\bar{z}}$ is the remaining lifetime of existing transmission line m connecting cities z and $\bar{z}$, and N_m is the lifetime of new transmission line m. Here, an existing transmission line m connecting cities z and $\bar{z}$ is considered to be composed of all the available transmission lines ms with the same voltage level between cities z and $\bar{z}$. Hence, $L_{m,z,\bar{z}}$ equals the maximum remaining lifetime of the existing transmission lines ms connecting cities z and $\bar{z}$, namely $L_{m,z,\bar{z}} = \max\left[L^{ms}_{m,z,\bar{z}}\right]$. The capacity of existing transmission line m over $L_{m,z,\bar{z}}$ should be determined by aggregating the capacities of all the existing transmission lines ms over their respective remaining lifetime.

- Useful operation years of transmission lines mx for importing electricity to city z installed in year n during a given planning horizon:

$$J_{mx,z,n}\begin{cases}(mx,z,n)\mid_{n=0} & y\geq 1, y\leq \min\left[L_{mx,z},Y\right]\\ (mx,z,n)\mid_{n\geq 1} & y\geq 1, y\leq \min\left[N_{mx}+n-1,Y\right]\end{cases} \tag{S10}$$

where $n = 0$ denotes the installation year of existing transmission lines for importing electricity, $L_{mx,z}$ is the remaining lifetime of existing transmission line mx for importing electricity to city z, and N_{mx} is the lifetime of new transmission line mx.

S3.1 Symbol definition

Symbols for model formulation	
Sets and indices	
G	generation technologies indexed by g
G_{FM}	firm generation technologies indexed by g
G_{FS}	fossil-based generation technologies indexed by g
G_{VRE}	variable renewable energy technologies indexed by g
S	storage technologies indexed by s
Z	cities in a region indexed by z and $\bar{z}$
M, MX	transmission lines indexed by m and mx
HM	hours in a day indexed by h
YM	years in a given planning horizon indexed by y and n
$J_{e,z,n}$	useful operation years of energy technology e installed in city z year n
$J_{m,z,\bar{z},n}$	useful operation years of transmission line m connecting cities z and $\bar{z}$ installed in year n
$J_{mx,z,n}$	useful operation years of transmission line mx for importing electricity to city z installed in year n
Parameters	
r	discount rate
dr_y	discount factor in year y
η_g	conversion efficiency of generation technology g
η_s^c, η_s^d	charging and discharging efficiencies of storage technology s
λ_g	availability of generation technology g
μ_g	minimum generation level of generation technology g
σ_s	self-charging efficiency of storage technology s
κ_{max}	maximum electricity import ratio
Ω_d	number of design days of type d in a year
$\varphi_g^{min}, \varphi_g^{max}$	minimum and maximum capacity factors of generation technology g
$\rho_g^{up}, \rho_g^{dn}, \rho_g$	ramping rates of generation technology g
θ_{dem}, θ_g	reserve margin for power demand and dynamic reserve for variable renewable technology g
ε_g	emission factor of generation technology g, [ton/MWh]

ϵ_g	fuel conversion factor of generation technology g, [ton/MWh or m^3/MWh]
δ_m, δ_{mx}	energy loss factor of transmission line m and mx, [%/100 km]
β_{mx}	cost share fraction of building transmission line mx
$ds_{z,\bar{z}}, ls_{mx}$	line length of transmission line connecting cities z and $\bar{z}$ or line mx , [km]
$\tau_s^{min}, \tau_s^{max}, \tau_s$	storage duration of storage technology s, [hr]
$\Gamma_{g,y}$	fossil fuel availability for generation technology g in year y, [ton or m^3]
$\Pi_{g,z}$	potential capacity of renewable technology g in city z, [MW]
E_z^{bio}	biomass potential of city z, [MWh]
$E_{z,dem}^{y,h}$	electricity demand of city z in year y hour h, [MWh]
$K_{e,n}^{CAP}$	capital cost of energy technology e in year n, [USD/MW]
$K_{e,y}^{FOM}$	fixed O&M cost factor of energy technology e in year y, [USD/MW]
$K_{e,y}^{VOM}$	variable O&M cost factor for energy technology e in year y, [USD/MWh]
$K_{g,y}^{fuel}$	price of fossil fuel for generation technology g in year y, [USD/MWh]
$K_{m,n}^{CAP}, K_{mx,n}^{CAP}$	capital cost of transmission line m and mx in year n, [USD/MW]
$K_{m,y}^{FOM}, K_{mx,y}^{FOM}$	fixed O&M cost factor of transmission line m and mx in year y, [USD/MW]
$K_{m,y}^{VOM}$	variable O&M cost factor of transmission line m in year y, [USD/MWh]
$K_{z,im}^{y,h}$	price of electricity imported to city z in year y hour h, [USD/MWh]
N_e, N_m, N_{mx}	lifetime of energy technology and transmission line, [yr]
$L_{e,z}, L_{m,z,\bar{z}}, L_{mx,z}$	remaining lifetime of energy technology and transmission line, [yr]
$P_{e,z,y}^{exn}$	capacity of existing energy technology e in city z year y, [MW]
$P_{e,z}^{min}, P_{e,z}^{max}$	minimum and maximum capacities of energy technology e for installation in city z, [MW]
$E_{s,z}^{min}, E_{s,z}^{max}$	minimum and maximum energy capacities of storage technology e for installation in city z, [MWh]
$\bar{F}_{m,z,\bar{z},y}^{exn}$	capacity of existing transmission line m connecting cities z and $\bar{z}$ in year y, [MW]
$\bar{F}_{mx,z,y}^{exn}$	capacity of existing transmission line mx for importing electricity to city z in year y, [MW]
$\bar{F}_{m,z,\bar{z}}^{min}, \bar{F}_{m,z,\bar{z}}^{max}$	minimum and maximum capacities of transmission line m for installation between cities z and z, [MW]
$\bar{F}_{mx,z}^{min}, \bar{F}_{mx,z}^{max}$	minimum and maximum capacities of transmission line mx for importing electricity to city z, [MW]
GHG_y^{max}	carbon emission limitation of year y, [ton]

Positive variables

$P_{e,z,n}^{nom}$	nominal capacity of energy technology e installed in city z year n, [MW]
$P_{e,z,n,y}^{nom}$	capacity of energy technology e installed in city z year n available in year y, [MW]
$P_{g,z,n,y}^{dnm}$	capacity of generation technology g installed in city z year n decommissioned in year y, [MW]
$\bar{F}_{m,z,\bar{z},n}^{nom}$	nominal capacity of transmission line m connecting cities z and $\bar{z}$ installed in year n, [MW]
$\bar{F}_{mx,z,n}^{nom}$	nominal capacity of transmission line mx for importing electricity to city z installed in year n, [MW]
$E_{s,z,n}^{nom}$	nominal energy capacity of storage technology s installed in city z year n, [MWh]
$P_{g,z,n}^{y,h}$	power produced by generation technology g installed in city z year n in time y, h, [MWh]

$F^{y,h}_{g,z,n}$	fuel consumed by by generation technology g installed in city z year n in time y, h, [MWh]
$C^{y,h}_{s,n,z}, D^{y,h}_{s,n,z}$	charging and discharging power of storage technology s installed in city z year n in time y, h, [MWh]
$E^{y,h}_{s,n,z}$	energy stored by storage technology s installed in city z year n in time y, h, [MWh]
$R^{y,h}_{e,z}$	operating reserve of energy technology e in city z in time y, h, [MW]
$\bar{F}^{y,h}_{m,z,\bar{z},n}$	power flow of transmission line m from city z to $\bar{z}$ installed in year n in time y, h, [MWh]
$\bar{F}^{y,h}_{mx,z,n}$	power flow of transmission line mx to city z installed in year n in time y, h, [MWh]
$P^{y,h}_{z,im}$	electricity imported to city z in time y, h, [MWh]
CEM_y	carbon emissions of year y, [ton]
TSC	total system costs, [USD]

S3.2 Objective function

The objective of low-carbon transition of power systems is to minimize total system costs (TSC), consisting of capital expenditure (CapEx), fuel costs (FCS), fixed operation and maintenance (FOM) costs, variable operation and maintenance (VOM) costs, and costs of importing electricity (CME) over a given planning horizon, as shown in Eq. (S11). A discount factor [$dr_y = (1 + r)^{-y}$] is used to convert future costs to present value via a discount rate (r). Moreover, since transmission lines for importing electricity are jointly built with other provinces, GHM region assumes only a certain fraction (β_{mx}) of their capital expenditure as well as operation and maintenance costs.

$$
\min\ TSC = \begin{cases}
\sum_{z\in Z}\sum_{g\in G}\sum_{n\geq 1} dr_n K^{CAP}_{g,n} P^{nom}_{g,n,z} + \sum_{g,z,n,y\in J_{g,z,n}} dr_y K^{FOM}_{g,y} P^{nom}_{g,z,n,y} \\
+ \sum_{z\in Z}\sum_{s\in S}\sum_{n\geq 1} dr_n K^{CAP}_{s,n} P^{nom}_{s,z,n} + \sum_{s,z,n,y\in J_{s,z,n}} dr_y K^{FOM}_{s,y} P^{nom}_{s,z,n,y} \\
+ \sum_{m\in M}\sum_{z<\bar{z}}\sum_{n\geq 1} dr_n K^{CAP}_{m,n} \bar{F}^{nom}_{m,z,\bar{z},n} + \sum_{m,z,\bar{z},n,y\in J_{m,z,\bar{z},n}} dr_y K^{FOM}_{m,y} \bar{F}^{nom}_{m,z,\bar{z},n,y} \\
+ \sum_{mx\in MX}\sum_{z\in Z}\sum_{n\geq 1} dr_n \beta_{mx} K^{CAP}_{mx,n} \bar{F}^{nom}_{mx,z,n} + \sum_{mx,z,n,y\in J_{mx,z,n}} dr_y \beta_{mx} K^{FOM}_{mx,y} \bar{F}^{nom}_{mx,z,n,y} \\
+ \sum_{g,z,n,y\in J_{g,z,n}}\sum_{h\in HM} dr_y \Omega_d \left(K^{VOM}_{g,y} + K^{fuel}_{g,y}/\eta_g\right) P^{y,h}_{g,z,n} \\
+ \sum_{s,z,n,y\in J_{s,z,n}}\sum_{h\in HM} dr_y \Omega_d K^{VOM}_{s,y} \left(C^{y,h}_{s,z,n} + D^{y,h}_{s,z,n}\right) \\
+ \sum_{m,z,\bar{z},n,y\in J_{m,z,\bar{z},n}}\sum_{h\in HM} dr_y \Omega_d K^{VOM}_{m,y} \left(\bar{F}^{y,h}_{m,z,\bar{z},n} + \bar{F}^{y,h}_{m,\bar{z},z,n}\right) \\
+ \sum_{z\in Z}\sum_{y\in YM}\sum_{h\in HM} dr_y \Omega_d K^{y,h}_{z,im} P^{y,h}_{z,im}
\end{cases}
\tag{S11}
$$

S3.3 Constraints

The low-carbon transition of power systems has to ensure that the hourly electricity demand is always satisfied during a given planning horizon. The system design and operation should be constrained by a series of equations consisting of capacity sizing, operation boundaries of energy technologies and transmission lines, electricity balance and system reliability, as well as imposed energy

policies and criterion. It is worth mentioning that the capacities of existing generation and storage technologies as well as transmission lines should be directly carried into optimization as they have been installed before system planning.

S3.3.1 Capacity sizing

The power capacity ($P^{nom}_{g,z,n}$) of a generation technology g installed in city z year n should be constrained to lie between $P^{min}_{g,z}$ and $P^{max}_{g,z}$.

$$P^{nom}_{g,z,n} \leq P^{max}_{g,z} \quad \forall g, z, n \geq 1 \tag{S12}$$

$$P^{nom}_{g,z,n} \geq P^{min}_{g,z} \quad \forall g, z, n \geq 1 \tag{S13}$$

The energy and power capacity ($E^{nom}_{s,z,n}$ and $P^{nom}_{s,z,n}$) of a storage technology s installed in city z year n should be constrained as follows:

$$E^{nom}_{s,z,n} \leq E^{max}_{s,z} \quad \forall s, z, n \geq 1 \tag{S14}$$

$$E^{nom}_{s,z,n} \geq E^{min}_{s,z} \quad \forall s, z, n \geq 1 \tag{S15}$$

$$P^{nom}_{s,z,n} \leq P^{max}_{s,z} \quad \forall s, z, n \geq 1 \tag{S16}$$

$$P^{nom}_{s,z,n} \geq P^{min}_{s,z} \quad \forall s, z, n \geq 1 \tag{S17}$$

The energy-to-power ratio of a storage technology can be constrained to lie within given ranges using minimum and maximum storage duration (τ^{min}_s and τ^{max}_s).

$$P^{nom}_{s,z,n}\tau^{max}_s \leq E^{nom}_{s,z} \quad \forall s, z, n \geq 1 \tag{S18}$$

$$P^{nom}_{s,z,n}\tau^{min}_s \geq E^{nom}_{s,z} \quad \forall s, z, n \geq 1 \tag{S19}$$

The power capacity ($\bar{F}^{nom}_{m,z,\bar{z},n}$) of a transmission line m connecting cities z and $\bar{z}$ installed in year n should be constrained as follows:

$$\bar{F}^{nom}_{m,z,\bar{z},n} \leq \bar{F}^{max}_{m,z,\bar{z}} \quad \forall m, z < \bar{z}, n \geq 1 \tag{S20}$$

$$\bar{F}^{nom}_{m,z,\bar{z},n} \geq \bar{F}^{min}_{m,z,\bar{z}} \quad \forall m, z < \bar{z}, n \geq 1 \tag{S21}$$

$$\bar{F}^{nom}_{m,z,\bar{z},n} = 0, \forall m, z \geq \bar{z}, n \geq 1 \tag{S22}$$

The power capacity ($\bar{F}^{nom}_{mx,z,n}$) of a transmission line mx for importing electricity to city z installed in year n is constrained as follows:

$$\bar{F}^{nom}_{mx,z,n} \leq \bar{F}^{max}_{mx,z} \quad \forall mx, z, n \geq 1 \tag{S23}$$

$$\bar{F}^{nom}_{mx,z,n} \geq \bar{F}^{min}_{mx,z} \quad \forall mx, z, n \geq 1 \tag{S24}$$

It is worth mentioning that Eqs. (S13, S15, S17, S21, and S24) are not used in this work to allow free selection of energy technologies and transmission lines. Moreover, $\tau^{min}_s = \tau^{max}_s = \tau_s$ is applied

to every storage technology to correlate its power and energy capacities, thus rendering Eq. (S14) unnecessary for storage technology modeling. Specifically, τ_s takes values of 12 hours for PSH and 4 hours for LiB. Furthermore, if existing generation and storage technologies and transmission lines have useful lifetime during given planning horizon, their capacities are directly carried into system planning.

S3.3.2 Operation boundaries

Generation technologies. The generation technologies are modeled by their availability (λ_g), conversion efficiencies (η_g), and minimum generation levels (μ_g). The hourly electricity generation can be determined using input fuel ($F^{y,h}_{g,z,n}$) and constrained as follows:

$$P^{y,h}_{g,z,n} = \eta_g F^{y,h}_{g,z,n} \leq \lambda_g P^{nom}_{g,z,n,y} \quad \forall h, g, z, n, y \in J_{g,n,z} \tag{S25}$$

$$P^{y,h}_{g,n,z} = \eta_g F^{y,h}_{g,n,z} \geq \lambda_g \mu_g P^{nom}_{g,z,n,y} \quad \forall h, g, z, n, y \in J_{g,n,z} \tag{S26}$$

where μ_g is a user-defined parameters and can be set by users according to their preferences and specific generation technologies, and μ_g is assumed to be zero in this work to model on-off operations of generation technologies. $P^{nom}_{g,z,n,y}$ denotes the capacity of generation technology g installed in city z year n available in year y and is expressed as follows:

$$P^{nom}_{g,z,n,y} = \begin{cases} P^{exn}_{g,z,y} & n = 0, y = 1 \text{ for existing technologies} \\ P^{nom}_{g,z,n} & n \geq 1, y = n \text{ for new installed technologies} \end{cases} \tag{S27}$$

where $P^{exn}_{g,z,y}$ indicates the capacity of existing technology g in city z year y, and we introduce $P^{dnm}_{g,z,n,y}$, which denotes the capacity decommissioned in the end of year y for technology g installed in city z year n, to model generation technology decommission as follows:

$$P^{nom}_{g,z,n,y+1} = P^{nom}_{g,z,n,y} - P^{dnm}_{g,z,n,y} \quad \forall g, z, n, y \in J_{g,z,n} \tag{S28}$$

$$P^{nom}_{g,z,n,y} \leq P^{exn}_{g,z,y} \quad \forall g, z, n = 0, y \in J_{g,z,n} \tag{S29}$$

Here, we consider free capacity decommission for only existing generation technologies.

A generation technology g cannot always run at its maximum capacity through a year, since it needs to be shut down for a certain period due to maintenance or a lack of generation resources. The generation of a technology g should be also no less than a threshold value within a year due to operation constraints or policy regulation. Here, we use minimum and maximum capacity factors (φ^{min}_g and φ^{max}_g) to enforce these constraints for generation technologies via Eq. (S30), where Ω_d denotes the number of design days of type d in a year.

$$\varphi^{min}_g \lambda_g P^{nom}_{g,z,n,y} \leq \sum_{h \in HM} \Omega_d P^{y,h}_{g,z,n} / 8760 \leq \varphi^{max}_g \lambda_g P^{nom}_{g,z,n,y} \quad \forall h, g, z, n, y \in J_{g,z,n} \tag{S30}$$

The generation change of a technology g in two consecutive hours in a year should be constrained

by its allowable upward and downward ramping rates (ρ_g^{up} and ρ_g^{dn}) to ensure safe operation.

$$P_{g,z,n}^{y,h} - P_{g,z,n}^{y,h-1} \leq \rho_g^{up} P_{g,z,n,y}^{nom} \quad \forall h > 1, g, z, n, y \in J_{g,z,n} \tag{S31}$$

$$P_{g,z,n}^{y,h} - P_{g,z,n}^{y,h-1} \geq -\rho_g^{dn} P_{g,z,n,y}^{nom} \quad \forall h > 1, g, z, n, y \in J_{g,z,n} \tag{S32}$$

Moreover, to account for ramping rate limitation, the operation status of a generation technology between the first hour of a year and the final hour of the previous year should satisfy Eqs. (S33-S34).

$$P_{g,z,n}^{y,1} - P_{g,z,n}^{y-1,H} \leq \rho_g^{up} P_{g,z,n,y}^{nom} \quad \forall y > 1, g, z, n, y \in J_{g,z,n} \tag{S33}$$

$$P_{g,z,n}^{y,1} - P_{g,z,n}^{y-1,H} \geq -\rho_g^{dn} P_{g,z,n,y}^{nom} \quad \forall y > 1, g, z, n, y \in J_{g,z,n} \tag{S34}$$

Here, upward and downward ramping rates of a generation technology are considered as the same ($\rho_g^{up} = \rho_g^{dn} = \rho_g$).

Firm generation technologies (excluding photovoltaics and wind turbines) need to provide reserves to cover unforeseen peaks in energy demand. The reserve provided by a generation technology g in city z should be constrained by its hourly generation, availability, and ramping rate as follows:

$$R_{g,z}^{y,h} \leq \sum_{n \leq y} \left(\lambda_g P_{g,z,n,y}^{nom} - P_{g,z,n}^{y,h} \right) \quad \forall h, g, z, n, y \in J_{g,z,n} \tag{S35}$$

$$R_{g,z}^{y,h} \leq \sum_{n \leq y} \rho_g P_{g,z,n,y}^{nom} \quad \forall h, g, z, n, y \in J_{g,z,n} \tag{S36}$$

Generation resource availability. Besides constraining by Eqs. (S25-S36), solar, wind, biomass and fossil-based generations are also subject to their resource availability. The accumulative capacity of solar and onshore wind in a city or offshore wind near a city needs to be constrained by their respective potentials ($\Pi_{g,z}$) as their installations are subject to space limitation.

$$\sum_{n \leq y} P_{g,z,n,y}^{nom} \leq \Pi_{g,z} \quad \forall g, z, n, y \in J_{g,z,n} \tag{S37}$$

The availability of coal and natural gas has a great impact on system expansion planning. Here, we constrain coal and natural gas resources for GHM region as follows:

$$\sum_{z \in Z} \sum_{n \leq y} \sum_{h \in HM} \epsilon_g \Omega_d F_{g,z,n}^{y,h} \leq \Gamma_{g,y} \quad \forall g, z, n, y \in J_{g,z,n} \tag{S38}$$

where ϵ_g is a conversion factor, and $\Gamma_{g,y}$ denotes coal and natural gas availability in year y. The annual biomass consumption in each city should be less than its biomass potential (E_z^{bio}) as follows:

$$\sum_{n \leq y} \sum_{h \in HM} \Omega_d F_{g,z,n}^{y,h} \leq E_z^{bio} \quad \forall g, z, n, y \in J_{g,z,n} \tag{S39}$$

Storage technologies. The storage technologies serve to balance spatial and temporal mismatch between power production and demand. The stored energy ($E_{s,n,z}^{y,h}$) as well as charging and discharging

behavior ($C^{y,h}_{s,n,z}$ and $D^{y,h}_{s,n,z}$) of a storage technology s can be described by Eq. (S40), where σ_s is the self-charging factor and η^c_s and η^d_s are the charging and discharging efficiencies.

$$E^{y,h}_{s,n,z} = E^{y,h-1}_{s,n,z}\,(1-\sigma_s) + \eta^c_s C^{y,h}_{s,n,z} - \frac{D^{y,h}_{s,n,z}}{\eta^d_s} \quad \forall h \geq 1, s, n, z, y \in J_{s,n,z} \tag{S40}$$

The energy stored at the beginning of a year should be linked to the energy stored at the end of the previous year. Moreover, the initial and final states of a storage technology should be the same as assured by Eq. (S42), where *yn* and *ym* denote the first and final useful operation years of a storage technology during its lifetime. It is worth noting that if $n = 0$, then $yn = 1$ and $ym = \min[L_{s,z}, Y]$; otherwise, $yn = n$ and $ym = \min[N_s + n - 1, Y]$.

$$E^{y,0}_{s,z,n} = E^{y-1,H}_{s,z,n} \quad \forall y > 1, s, z, n, y \in J_{s,z,n} \tag{S41}$$

$$E^{yn,0}_{s,z,n} = E^{ym,H}_{s,z,n} \quad \forall s, z, n, yn, ym \in J_{s,z,n} \tag{S42}$$

A storage technology has to work within its allowable performance boundary for safe operation. Hence, hourly charging, discharging and stored energy should be constrained by its availability (λ_s) and power and energy capacities as follows:

$$C^{y,h}_{s,z,n} \leq \lambda_s P^{nom}_{s,z,n,y} \quad \forall h, s, z, n, y \in J_{s,z,n} \tag{S43}$$

$$D^{y,h}_{s,z,n} \leq \lambda_s P^{nom}_{s,z,n,y} \quad \forall h, s, n, z, y \in J_{s,z,n} \tag{S44}$$

$$E^{y,h}_{s,z,n} \leq E^{nom}_{s,z,n,y} = \tau_s P^{nom}_{s,z,n,y} \quad \forall h, s, z, n, y \in J_{s,z,n} \tag{S45}$$

where $P^{nom}_{s,z,n,y}$ denotes the capacity of storage technology s installed in city z year n available in year y and is expressed as follows:

$$P^{nom}_{s,z,n,y} = \begin{cases} P^{exn}_{s,z,y} & n = 0 \text{ for existing technologies} \\ P^{nom}_{s,z,n} & n \geq 1 \text{ for new installed technologies} \end{cases} \tag{S46}$$

Here, $P^{exn}_{s,z,y}$ represents the capacity of existing storage technology s in city z year y. Simultaneous charging and discharging may occur for storage technologies during system optimization. Eliminating simultaneous charging and discharging in all situations normally requires constraints with binary variables to force charging power to be zero whenever discharging power is nonzero and vice versa. However, introducing binary constraints incurs expensive computational burden. To avoid this issue and maintain a tractable linear formulation, we introduce Eq. (S47).

$$C^{y,h}_{s,z,n} + D^{y,h}_{s,z,n} \leq \lambda_s P^{nom}_{s,z,n,y} \quad \forall h, s, z, n, y \in J_{s,z,n} \tag{S47}$$

Moreover, a VOM cost term that accounts for charging and discharging costs using an economic factor can be added to the objective function for eliminating simultaneous charging and discharging as can be seen in Eq. (S11).

Storage technologies should also provide reserve to help satisfy unforeseen peak demand. The

reserve provided by storage technology s in city z should be constrained by its hourly charging and discharging power, stored energy and power capacity as follows:

$$R^{y,h}_{s,z} \leq \sum_{n \leq y} \left(\eta^d_s \lambda_s P^{nom}_{s,z,n,y} - D^{y,h}_{s,z,n} \right) \quad \forall h, s, z, n, y \in J_{s,z,n} \tag{S48}$$

$$R^{y,h}_{s,z} \leq \sum_{n \leq y} \eta^d_s \left(E^{y,h-1}_{s,z,n} + \eta^c_s C^{y,h}_{s,z,n} - \frac{D^{y,h}_{s,z,n}}{\eta^d_s} \right) \quad \forall h \geq 1, s, z, n, y \in J_{s,z,n} \tag{S49}$$

Transmission lines. The power flow along a transmission line m connecting cities z and $\bar{z}$ should be constrained by Eqs. (S50-S51), where a loss factor (δ_m) and line length between cities ($ds_{z,\bar{z}}$) are used to determine power losses during transmission. The transmission capacity of bidirectional power transmission between cities z and $\bar{z}$ is assumed the same in this work.

$$\bar{F}^{y,h}_{m,z,\bar{z},n} (1 - \delta_m ds_{z,\bar{z}}) \leq \bar{F}^{nom}_{m,z,\bar{z},n,y} \quad \forall h, m, z, \bar{z}, n, y \in J_{m,z,\bar{z},n} \tag{S50}$$

$$\bar{F}^{y,h}_{m,\bar{z},z,n} (1 - \delta_m ds_{z,\bar{z}}) \leq \bar{F}^{nom}_{m,z,\bar{z},n,y} \quad \forall h, m, z, \bar{z}, n, y \in J_{m,z,\bar{z},n} \tag{S51}$$

where $\bar{F}^{nom}_{m,z,\bar{z},n,y}$ denotes the capacity of transmission line m connecting cities z and $\bar{z}$ installed in year n available in year y and is determined as follows:

$$\bar{F}^{nom}_{m,z,\bar{z},n,y} = \begin{cases} \bar{F}^{exn}_{m,z,\bar{z},y} & n = 0 \text{ for existing tranmission lines} \\ \bar{F}^{nom}_{m,z,\bar{z},n} & n \geq 1 \text{ for new installed tranmission lines} \end{cases} \tag{S52}$$

Here, $\bar{F}^{exn}_{m,z,\bar{z},y}$ represents the capacity of existing transmission line m connecting cities z and $\bar{z}$ in year y. Bidirectional power flow along transmission lines may occur during system optimization. Similar to Eq. (S47), we introduce Eq. (S53) and use a cost factor associated with power transmission to inhibit bidirectional power flows without significantly affecting system O&M costs as can be found in Eq. (S11).

$$\left(\bar{F}^{y,h}_{m,z,\bar{z},n} + \bar{F}^{y,h}_{m,\bar{z},z,n} \right) (1 - \delta_m ds_{z,\bar{z}}) \leq \bar{F}^{nom}_{m,z,\bar{z},n,y} \quad \forall h, m, z, \bar{z}, n, y \in J_{m,z,\bar{z},n} \tag{S53}$$

The electricity imported from other provinces ($\bar{F}^{y,h}_{mx,z,n}$) to city z using transmission line mx should be constrained by its available capacity ($\bar{F}^{nom}_{mx,z,n,y}$) as follows:

$$\bar{F}^{y,h}_{mx,z,n} (1 - \delta_{mx} ls_{mx}) \leq \bar{F}^{nom}_{mx,z,n,y} \quad \forall h, mx, z, n, y \in J_{mx,z,n} \tag{S54}$$

$$\bar{F}^{nom}_{mx,z,n,y} = \begin{cases} \bar{F}^{exn}_{mx,z,y} & n = 0 \text{ for existing tranmission lines} \\ \bar{F}^{nom}_{mx,z,n} & n \geq 1 \text{ for new installed tranmission lines} \end{cases} \tag{S55}$$

where δ_{mx} is a loss factor for power transmission, ls_{mx} denotes the length of transmission line mx, and $\bar{F}^{exn}_{mx,z,y}$ represents the capacity of existing transmission line mx for importing electricity in year y. The

total electricity imported to city z can be determined as follows:

$$P_{z,im}^{y,h} = \sum_{n \le y} \bar{F}_{mx,z,n}^{y,h} \left(1 - \delta_{mx} ls_{mx}\right) \quad \forall h, mx, z, n, y \in J_{mx,z,n} \tag{S56}$$

S3.4 Electricity balance and system security

The electricity balance has to be maintained during low-carbon transition of power systems. The hourly electricity demand of each city equals the sum of electric power produced by generation technologies, discharged by storage technologies, transmitted from other cities, and imported from other provinces, and minus the sum of electricity stored by storage technologies and transmitted to other cities, as assured by Eq. (S57).

$$\begin{aligned} &\sum_{\substack{n \le y \\ g,z,n,y \in J_{g,z,n}}} P_{g,n,z}^{y,h} + \sum_{\substack{n \le y \\ s,z,n,y \in J_{s,z,n}}} \left(D_{s,z,n}^{y,h} - C_{s,z,n}^{y,h}\right) + P_{z,im}^{y,h} \\ &+ \sum_{\substack{n \le y \\ m,z,\bar{z},n,y \in J_{m,z,\bar{z},n}}} \left(\bar{F}_{m,\bar{z},z,n}^{y,h} \left(1 - \delta_m ds_{z,\bar{z}}\right) - \bar{F}_{m,z,\bar{z},n}^{y,h}\right) = E_{z,dem}^{y,h} \quad \forall y, h, z \end{aligned} \tag{S57}$$

The power system needs to provide sufficient reserve in order to cover unforeseen peak demands in each city during given planning horizon. The system reserve is determined by considering a reserve margin (θ_{dem}) for power demand and a dynamic reserve (θ_g) for variable renewable generation (solar and wind) to ensure operation reliability as follows:

$$\sum_{g \in G_{NVRE}} R_{g,z}^{y,h} + \sum_{s \in S} R_{s,z}^{y,h} \ge \theta_{dem} E_{z,dem}^{y,h} + \sum_{g \in G_{VRE}} \theta_g \sum_{\substack{n \le y \\ n,y \in J_{g,z,n}}} P_{g,z,n}^{y,h} \quad \forall y, h, z \tag{S58}$$

GHM region mainly imports hydropower from southwestern China. A high electricity import ratio can reduce generation investments; however, it leads to overreliance on external generation sources. This may incur huge economic loss when intense competition among regions for purchasing external electricity causes a sharp rise in electricity price. Hence, constraining annual imported electricity is beneficial for avoiding economic loss and guaranteeing system security. Having this in mind, annual imported electricity should be lower than a tolerable import ratio (κ_{max}) represented by a fraction of annual power demand as in Eq. (S59).

$$\sum_{z \in Z} \sum_{h \in HM} \Omega_d P_{z,im}^{y,h} \le \kappa_{max} \sum_{z \in Z} \sum_{h \in HM} \Omega_d E_{z,dem}^{y,h} \quad \forall y \tag{S59}$$

S3.5 Low-carbon transition pathways and performance indicators

The annual carbon emissions (CEM_y) of a power system sourced from fossil-based generations ($g \in G_{FS}$) can be obtained using their emission factors (ε_g) as follows:

$$CEM_y = \sum_{z\in Z} \sum_{\substack{n\le y, g\in G_{FS} \\ g,z,n\in J_{g,z,n}}} \sum_{h\in HM} \varepsilon_g \Omega_d F^{y,h}_{g,z,n} \le GHG^{max}_y \quad \forall y \tag{S60}$$

The optimal transition pathways of a power system can be determined by imposing an annual threshold of carbon emissions (GHG^{max}_y) for every year during a given planning horizon. Moreover, by summing Eq. (S60) with respective to every year, we can obtain $\sum_y CEM_y \le \sum_y GHG^{max}_y$, which indicates that cumulative carbon emissions during a given planning horizon are constrained by constant total emissions.

Average electricity cost (AEC) and average decarbonization cost (ADC) are two additional performance indicators used in this work for comparing different transition pathways. Here, AEC means the average costs a power system needs to pay for meeting electricity demand during given planning horizon.

$$AEC = \frac{TSC}{\sum_{z\in Z}\sum_{y\in YM}\sum_{h\in HM}\Omega_d E^{y,h}_{z,dem}} \tag{S61}$$

ADC refers to the additional costs a power system needs to pay for reducing one tone of carbon emissions between two scenarios. Numerically, ADC can be determined by dividing TSC difference between two scenarios by their carbon emission difference as follows:

$$ADC_{n,m} = \frac{TSC_n - TSC_m}{CBD_m - CBD_n} \tag{S62}$$

where TSC_n and CBD_n denote total system costs and carbon emissions during given planning horizon for scenario n, while TSC_m and CBD_m represent total system costs and carbon emissions during given planning horizon for reference scenario m. Here, ADC is computed with business-as-usual scenario as reference scenario.

S3.6 Solution strategy

The low-carbon transition of GHM power system is formulated as a large-scale linear programming (LP) problem with more than 9,270,000 equations and 5,000,000 variables. The LP problem is solved by Gurobi optimizer with a relative optimality gap of 0.1% and a maximum CPU time of 20 hours in GAMS. Primal-simplex, dual-simplex, and barrier algorithms can be used for solving LP problems. However, employing a single algorithm only may fail in this problem, since it contains massive extreme points, namely vertices in its feasible region. For this, we employ parallel computation strategy that effectively combines these algorithms in Gurobi optimizer for solving this LP problem. The computation platform is a DELL Precision T7920 workstation with 2 2.90 GHz Intel Xeon Gold 6226R CPUs, 128 GB RAM, and Windows 10 operating system.

Table S8 Capital costs of energy technologies in different years.[35–38]

	Technology [USD/kW]	2021	2025	2030	2035	2040	2045	2050
Clean energy generation	Solar PV	623	509	367	351	334	318	302
	Onshore wind	1,224	1,063	863	820	776	733	690
	Offshore wind	1,905	1,604	1,351	1,246	1,168	1,105	1,052
	Nuclear,	1,980	1,916	1,862	1,797	1,734	1,674	1,593
	Hydro	1,312	1,312	1,312	1,312	1,260	1,260	1,260
	Biomass	1,794	1,776	1,727	1,667	1,608	1,553	1,479
Fossil generation	CCGT	476	468	456	446	436	427	414
	CCGT-CCS	886	825	776	722	673	645	609
	Coal	571	562	531	504	487	470	448
	Coal-CCS	1,222	1,190	1,085	975	895	857	818
Energy storage	PSH	855	855	855	855	821	821	821
	LiB	1,282	956	784	735	686	637	588

Table S9 Fixed operation and maintenance (FOM) costs of energy technologies in different years.[37]

	Technology [USD/kW-yr]	2021	2025	2030	2035	2040	2045	2050
Clean energy generation	Solar PV	22.7	20.0	16.6	16.2	15.8	15.4	15.0
	Onshore wind	42.3	40.8	39.0	37.5	36.0	34.6	33.1
	Offshore wind	106.6	94.6	86.3	80.7	76.5	73.1	70.3
	Nuclear	145.0	145.0	145.0	145.0	145.0	145.0	145.0
	Hydro	63.3	63.3	63.3	63.3	60.7	60.7	60.7
	Biomass	149.8	149.8	149.8	149.8	149.8	149.8	149.8
Fossil generation	CCGT	27.3	27.3	27.3	27.3	27.3	27.3	27.3
	CCGT-CCS	65.1	64.4	63.3	61.7	60.4	60.4	60.4
	Coal	71.8	71.4	69.4	68.2	68.2	68.2	68.2
	Coal-CCS	122.3	121.1	115.3	109.1	105.0	105.0	105.0
Energy storage	PSH	17.6	17.6	17.6	17.6	17.6	17.6	17.6
	LiB	32.0	23.9	19.6	18.4	17.2	15.9	14.7

Table S10 Variable operation and maintenance (VOM) costs of energy technologies in different years.

	Technology [USD/MWh]	2021	2025	2030	2035	2040	2045	2050
Clean energy Generation[37]	Nuclear	2.35	2.35	2.35	2.35	2.35	2.35	2.35
	Biomass	4.79	4.79	4.79	4.79	4.79	4.79	4.79
Fossil generation[37]	CCGT	1.74	1.74	1.74	1.74	1.74	1.74	1.74
	CCGT-CCS	5.73	5.67	5.57	5.44	5.32	5.32	5.32
	Coal	7.86	7.8	7.52	7.35	7.35	7.35	7.35
	Coal-CCS	14.26	14.21	13.94	13.49	13.06	13.06	13.06
Energy storage	PSH[37]	0.51	0.51	0.51	0.51	0.51	0.51	0.51
	LiB[39]	3.0	3.0	3.0	3.0	3.0	3.0	3.0

S4 Model input data

The model input data includes capacities of existing generation and storage technologies, topology and capacities of existing transmission networks, electricity load profiles, potential capacities and capacity factors of renewable technologies, fuel and electricity prices, and technology cost and performance data. The first four terms has been discussed thoroughly in previous sections. The fuel

and electricity prices as well as technology cost and performance data are presented in detail in the following.

S4.1 Fuel and electricity prices

Gas-fired, coal-fired, and nuclear plants require fuels for power generation. The gas and coal prices vary significantly from provinces to provinces, as transportation costs account for a large proportion. The coal price is taken from Price Testing Center of National Development and Reform Commission (NRDC)[40], which provides detailed information on provincial coal prices in China. The gas price is also derived from NRDC's price reform notification[41], which presents non-residential gas price for each province in China. The uranium price for nuclear generation is adopted from 2021 Annual Technology Baseline[37], which provides nuclear fuel price projection from 2021 to 2050. GHM region faces substantial power deficits in recent decades due to its prosperous economy. Several west-to-east power transmission projects have been built for exporting hydropower from Sichuan, Yunnan, and Guangxi provinces to help satisfy GHG region's electricity demand. Ren and Han[42] analyzed the pricing mechanism of west-to-east power transmission projects, while Tao et al.[43] investigated hydropower potentials in Yunnan province and its average grid price of hydropower from 2021to 2025. We adopted these fuel and electricity prices in this work for planning GHM power system transition.

S4.2 Cost and performance data of energy technologies

The capital costs of solar, onshore wind, offshore wind, and fossil-based generation are mainly derived from Manual of Renewable Energy Data released by National Energy Administration[44] and Grid Project Construction Cost Analysis in the 11th Five-Year Period[45]. Chen et al.[15] provides a comprehensive review on capital costs of these energy technologies. The capital costs of nuclear, hydro, biomass, and storage technologies are mainly taken from China Power Industry Annual Development Report[46] and Annual Technology Baseline from National Energy Renewable Laboratory[37]. For these capital costs, we adopted medium cost projection in our main scenarios, as presented in Table S8, while low- and high-cost projections are used later in system sensitivity analysis. The fixed and variable O&M costs are mainly adopted from Annual Technology Baseline from National Energy Renewable Laboratory[37], as shown in Tables S9-S10. Moreover, we assume a discount rate (r) of 5%[37] in this work to change future costs to present day values.

The capital costs of power transmission lines are mainly obtained from Zhang et al.'s work[47], which provides detailed cost data for possible construction of power transmission lines in China. The fixed O&M costs of transmission lines are assumed to be 3.5% of their capital costs, since it is hard to find this data from open literature. Moreover, to eliminate bidirectional power transmission, a cost factor of 5.0 USD/MWh is used for assessing variable O&M costs of power transmission. The energy loss factors are assumed to be 1%/100 km for inter-city power transmission and 0.5%/100 km for west-to-east power transmission.

The operating characteristics of energy technologies are taken from Annual Energy Outlook[48], Zeyringer et al.'s work[29], and Annual Technology Baseline[37], as shown in Table S11. Integrating CCS technology with gas-fired and coal-fired generation can remove their carbon emissions by 90%[37]. We

adopt this data in this work to capture carbon emissions of fossil-based generation with CCS technology. Moreover, reserve margin (θ_{dem}) and dynamic reserve (θ_g) are set to 0.05 and 0.1, respectively to ensure operation reliability. Since electricity import ratio in GHM region reached 19.3% in 2021[49], we assume maximum electricity import ratio (κ_{max}) takes a value of 20% in this work to avoid over-reliance on external power sources and guarantee system security. Fossil fuel (coal and natural gas) availability has a great impact on GHM power system transition. The 14th Five-Year Energy Development Plan of Guangdong Province[3] announces to achieve coal and natural gas supply ability of 100 million ton per year and 80 billion cubic meters per year in 2025. We employ these data as fossil resource availability to constrain fossil fuel consumption during system optimization.

Table S11 Operating characteristics of energy technologies.[29,37,48]

Technology	Efficiency [η]	Availability [λ]	Ramping rate [ρ]	Capacity factor [φ^{min},φ^{max}]	Emissions [ton/MWh]	Lifetime [yr]
Solar PV	-	-	-	-	-	25
Onshore wind	-	-	-	-	-	20
Offshore wind	-	-	-	-	-	20
Nuclear	0.326	0.911	0.25	0.5, 0.9	-	30
Hydro	-	0.982	1.0	0.2, 0.78	-	40
Biomass	0.28	0.9	0.5	0.2, 0.83	-	25
CCGT	0.536	0.947	0.5	0, 0.87	0.1836	25
CCGT-CCS	0.477	0.947	0.5	0, 0.87	0.01836	25
Coal	0.403	0.95	0.35	0, 0.85	0.3132	40
Coal-CCS	0.315	0.95	0.35	0, 0.85	0.03132	40
PSH	0.8	0.9	1.0	-	-	50
LiB	0.85	0.9	1.0	-	-	15

S5 Model scenario descriptions

In this work, we explore optimal investment plans and operation characteristics for energy technologies and transmission networks under multiple scenarios to design cost-effective pathways for GHM power system decarbonization. The hourly load profiles of each city are obtained by prediction and scaling methods as described in Section S1.4. Since Macau is a very small city with low electricity demands, it is merged with its adjacent city (Zhuhai), and its load profiles are added into Zhuhai's load profiles.

System decarbonization scenarios. Various scenarios have been considered to explore optimal transition pathways for decarbonizing GHM power system. A business-as-usual (BAU) scenario is set up as base scenario, where fossil resources and carbon emissions are not constrained. Moreover, three decarbonization scenarios (CDM70, CDM85, CDM100) are designed for pathway exploration, as shown in Figure S8, corresponding to emission mitigation trends of China's power system under decarbonization scenarios of China's national determination contritions (NDC), global warming of 2.0 °C (GM2.0), and carbon neutrality in 2050 (CN50)[47]. The carbon emissions of GHM power system in 2020 reaches around 256 million ton[50]. Starting from this initial emissions, maximum annual carbon emissions decrease with time in each scenario from 2021 to 2050. To obtain their

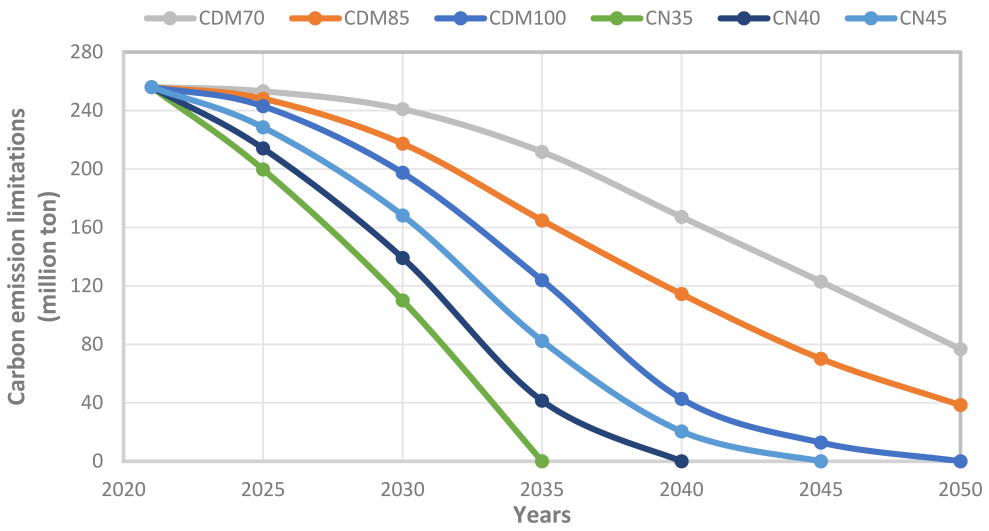

Figure S8 The annual carbon emission trajectories of different decarbonization scenarios for GHM power system.

emission trajectories, we normalize emission mitigation trends of China's power system under NDC, GM2.0, and CN50 scenarios[47], modify them slightly, and scale them by initial emissions of GHM power system. The three scenarios represent three carbon dioxide mitigation (CDM) levels relative to 2020 by 70%, 85%, and 100% in 2050 for GHM power system, and thus are named in this work as CDM70, CDM85, and CDM100. The three scenarios may not represent the optimal emission trajectories for GHM power system; however, they can at least guarantee that GHM power system decarbonization would not lag behind China's national decarbonization plan.

Furthermore, three ambitious scenarios (CN35, CN40, CN45) are designed to quantify the impacts of achieving carbon neutrality (CN) in 2030, 2040, and 2045 on GHM region. This indicates that carbon emissions of CN35 after 2035, CN40 after 2040, and CN45 after 2045 are all zero. We then follow CDM100's emission trajectory to design CN35, and equally divide the difference in carbon emissions between CN35 and CDM100 to obtain CN40 and CN45 emission trajectories.

Table S12 presents detailed descriptions of various decarbonization scenarios. GHM power system follows these designed emission trajectories with medium capital cost projection as mentioned in Section S4.2 towards low-carbon transition. We analyze how investments plans of generation and transmission capacities should be made and how hourly operations of energy technologies and transmission networks should be coordinated with each other to realize an economic and smooth transition.

System sensitivities. The decarbonization pathways may be significantly impacted by system parameters and energy policies. To unearth the effects of technology and fuel cost projections and energy policies on GHM power system, we develop another eight scenarios with varying capital costs of renewable (solar and wind) and storage technologies, prices of fossil fuels, electricity import ratio, discount rate, and electrification, as shown in Table S12. It is worth mentioning that HPF scenario uses price trajectory of U.S. fossil fuels[36], since it is very difficult to find fossil fuel price projection for GHM region. The U.S. fossil fuel price trajectory is normalized and then scaled by GHM fossil fuel prices in 2021 for sensitivity studies. These scenario analyses are performed for CDM70, CDM85, and CDM100, where annual power system emissions are constrained by maximum annual emission

values on their respective emission trajectories in Figure S8. This can be described by Eq. (S60), via implementing which cumulative carbon emissions during given planning horizon is constrained by constant total emissions. We aim to examine how sensitive these decarbonization pathways will be and how to make investment decisions for generation and transmission capacities.

Table S12 Scenario descriptions for decarbonization pathway exploration.

Abbreviation	Description
1. BAU	Meeting hourly power demand from 2021 to 2050 without fossil resources and carbon emissions limitation
2. Optimal Transition Pathways	
CDM70, CDM85, CDM100	Satisfying carbon emission limitation and hourly power demand by coordinating investment plans and operations of renewables, fossil and nuclear generations, storage systems, and electricity import for each city with all possible inter-city transmissions
3. Ambitious Transition Pathways towards Carbon Neutrality	
CN35, CN40, CN45	Achieving carbon neutrality in 2035, 2040, and 2045 under three emission trajectories
4. System Sensitivities on Cost Projection	
NTM	No transmission network expansion to showcase network expansion's importance
HFP	High fossil fuel (coal and natural gas) price trajectory (low availability of fossil fuels)[36]
HRS	High capital cost trajectories for renewable (solar and wind) and storage technologies[37,44]
LRS	Low capital cost trajectories for renewable (solar and wind) and storage technologies[37,44]
ECR	electricity demand increase according to eletrification trajectory[47]
LEI	Low electricity import ratio: 10% of system annual demand
HEI	High electricity import ratio: 30% of system annual demand
LSC	Low system costs: low capital cost trajectory for renewable and storage technologies + transmission network expansion + high electricity import ratio to provide a lower bound for system decarbonization

S6 Supplementary figures

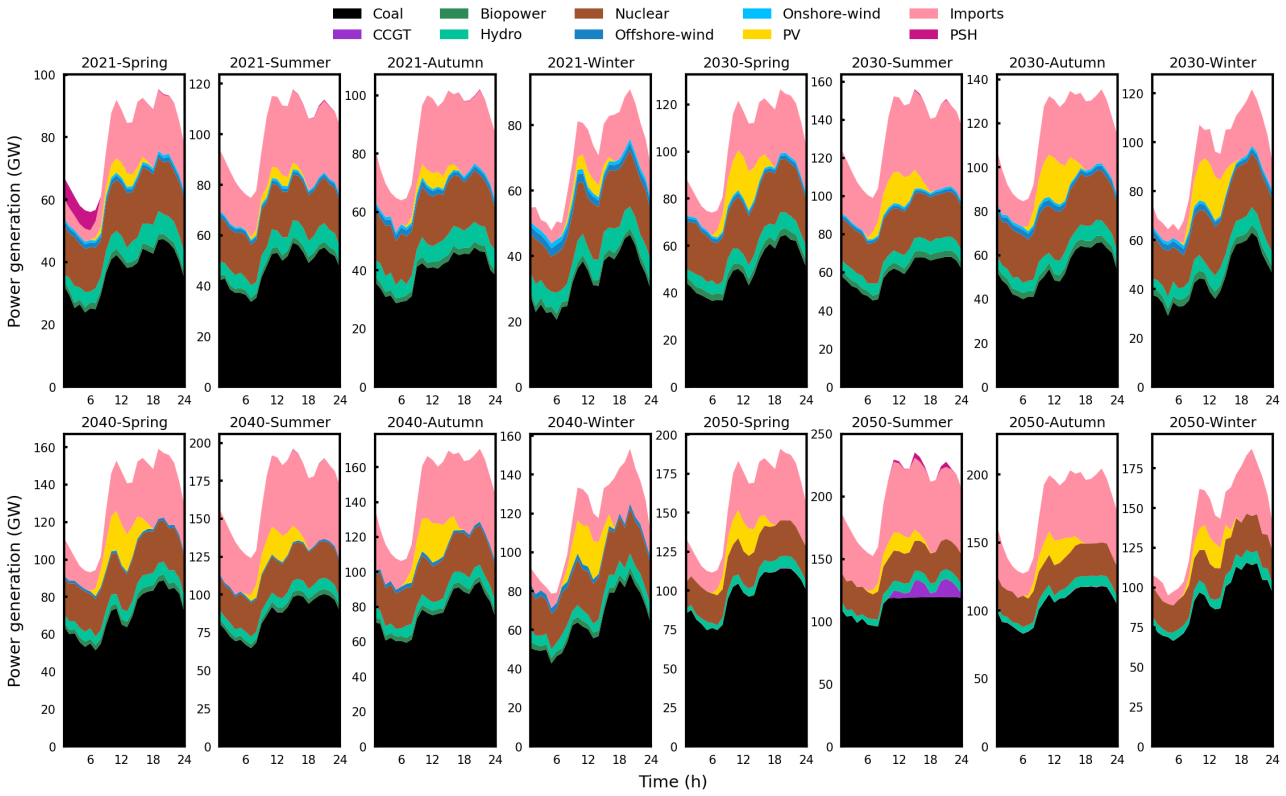

Figure S9 The hourly dispatches of energy technologies in spring, summer, autumn, and winter days in BAU scenario. Coal-fired generation dominates system power generation, and accounts for 46-60% of annual power demand between 2021 and 2050. PSH and CCGT run only in spring day in 2021 and summer day in 2050, and mainly serve as reserve providers. PV, onshore-wind, offshore-wind, hydro, and biomass generations are relatively low in BAU scenario.

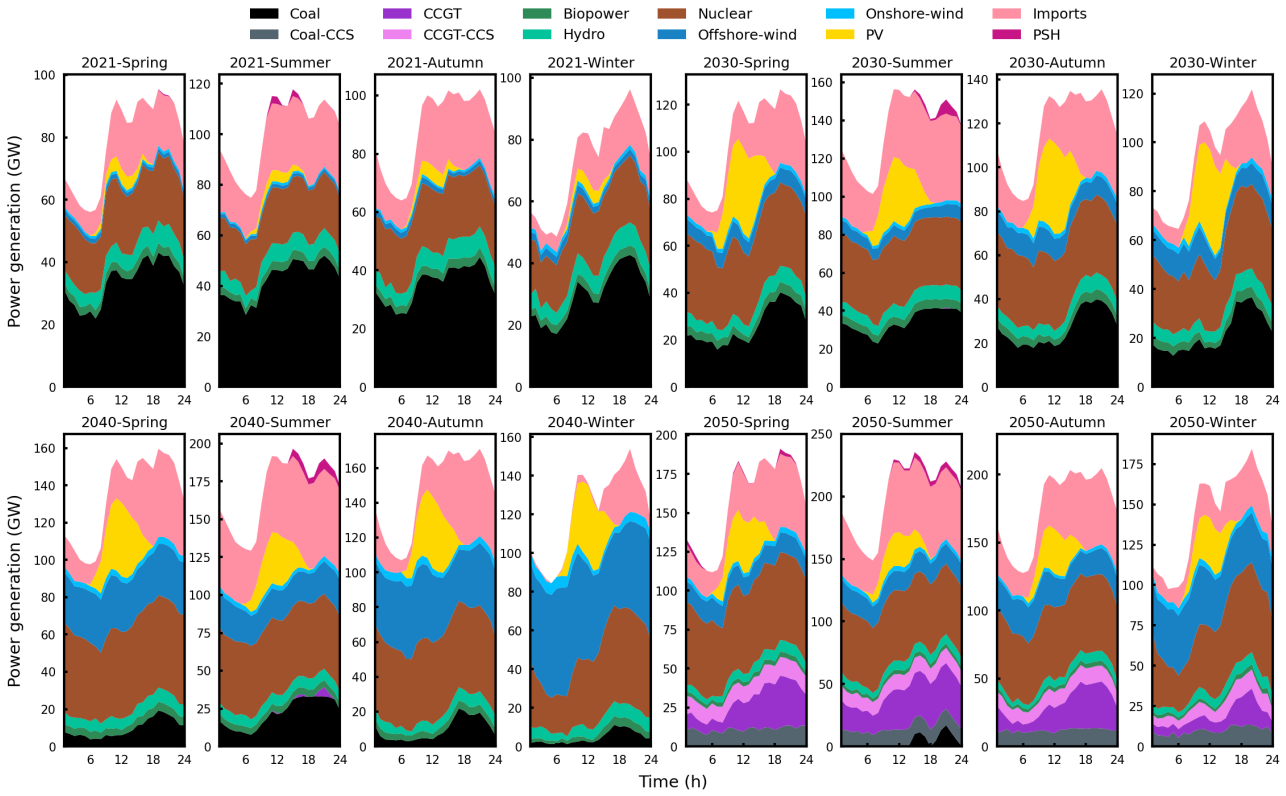

Figure S10 The hourly dispatches of energy technologies in spring, summer, autumn, and winter days in CDM70 scenario. Coal-fired generation decreases significantly from 309.8 TWh in 2021 to 7.5 TW in 2050. Offshore-wind generation peaks in 2040, especially in winter day, and then decreases gradually due to technology decommission. Coal-CCS, CCGT and CCGT-CCS can help meeting system emission limitation in 2050, and thus avoiding excess investments in renewable technologies.

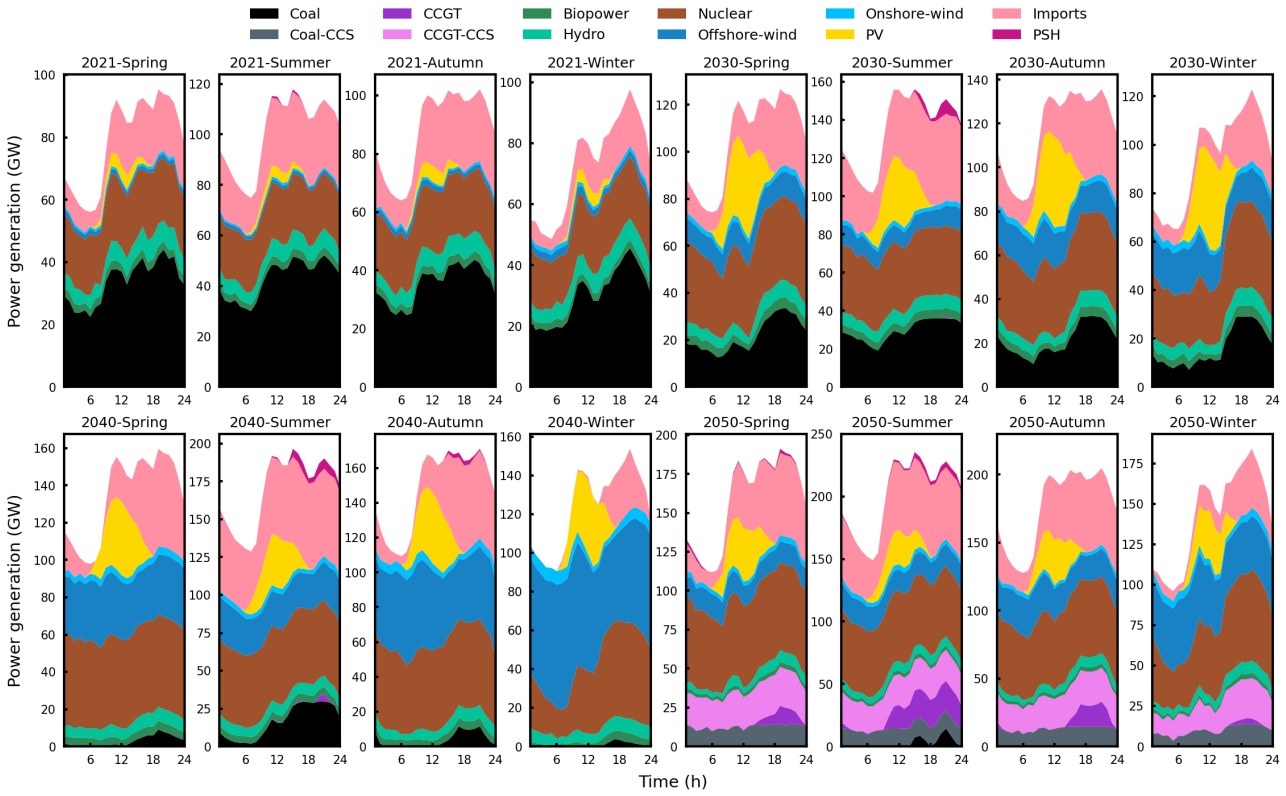

Figure S11 The hourly dispatches of energy technologies in spring, summer, autumn, and winter days in CDM85 scenario. Coal-fired generation decreases significantly from 312.0 TWh in 2021 to 5.4 TW in 2050. Offshore-wind generation peaks in 2040, especially in winter day, and then decreases gradually due to technology decommission. Coal-CCS, CCGT and CCGT-CCS can help meeting system emission limitation in 2050; however, Coal-CCS and CCGT-CCS play more important roles than CCGT on emission mitigation.

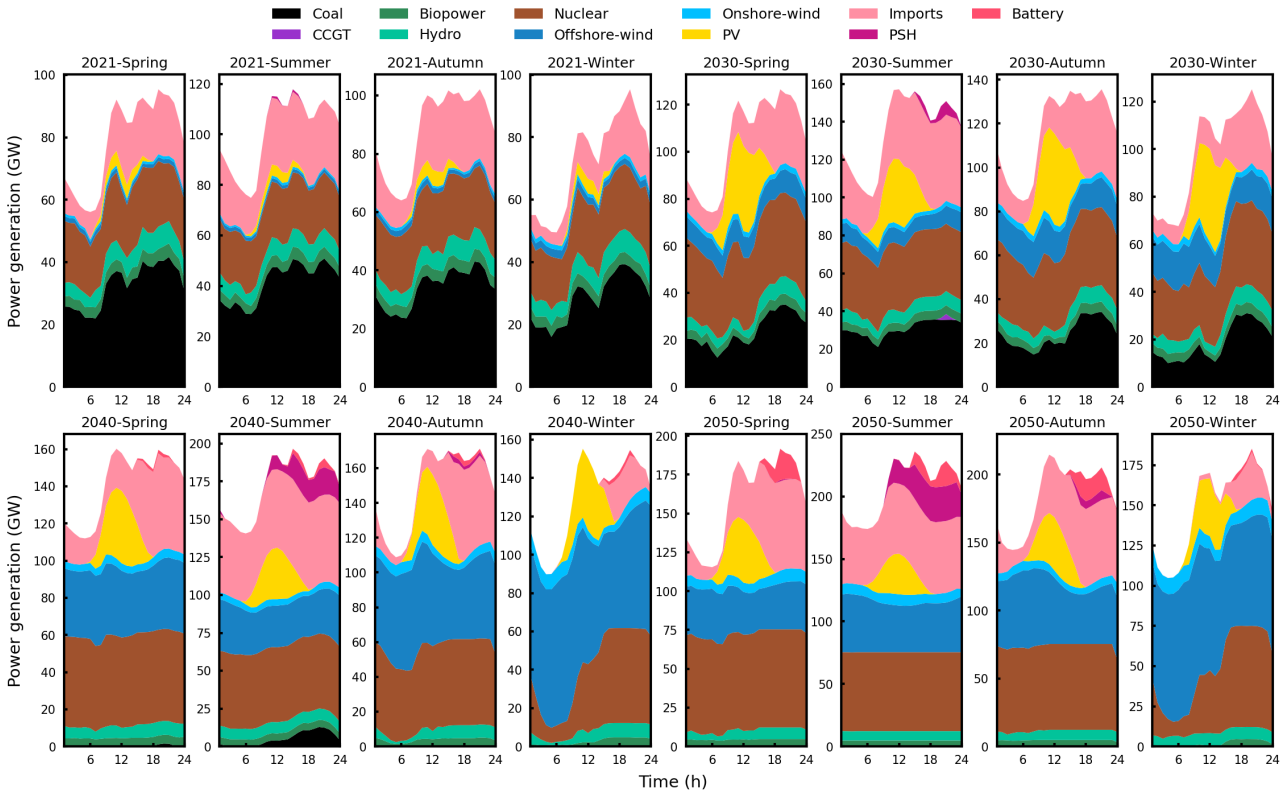

Figure S12 The hourly dispatches of energy technologies in spring, summer, autumn, and winter days in CDM100 scenario. Coal-fired generation decreases from 300.0 TWh in 2021 to zero in 2050. Offshore-wind and nuclear generation increases significantly to compensate power reduction from coal-fired generation. The hourly offshore-wind and nuclear generation in 2050 reaches 70.0 GW and 63.0 GW, respectively. PSH and li-ion battery are invested to balance offshore-wind intermittency. PSH and li-ion battery discharge power mainly in summer day after 2040 to meet peak power demand.

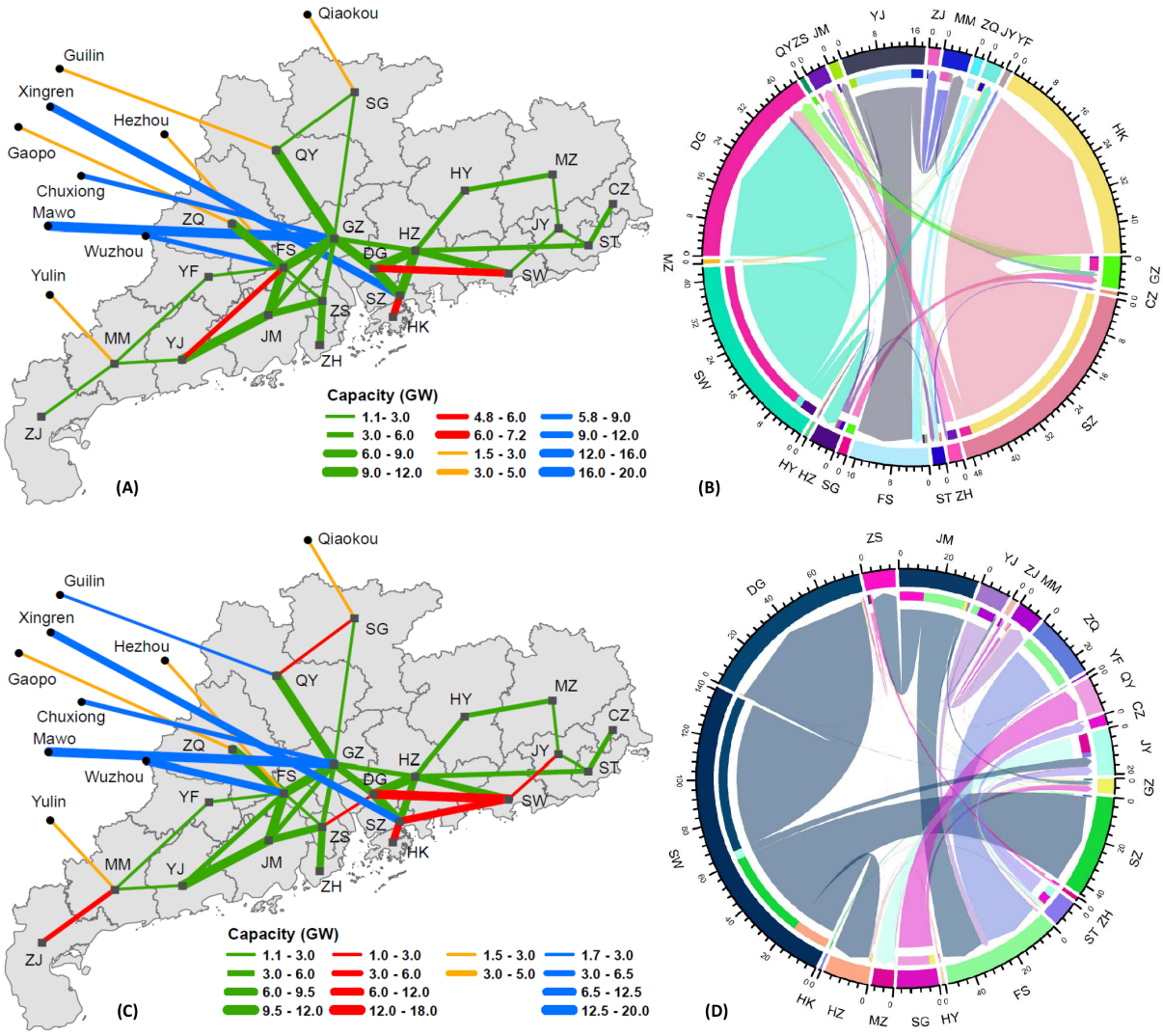

Figure S13 Optimal transmission networks (GW) and annual power flows (TWh) of GHM power system in 2050: (A-B) BAU and (C-D) CDM70. (A and C) The yellow and green lines denote existing transmission lines for electricity import and inter-city power transmission, respectively. The blue lines indicate reinforced transmission lines for importing electricity, while the red lines represent reinforced transmission lines for power transmission between cities. (B and D) The node sections denote the total exchanged power. The chord inside the circle indicates the transmitted power, the color denotes destination on node section, and the arrow represents power flow direction between cites.

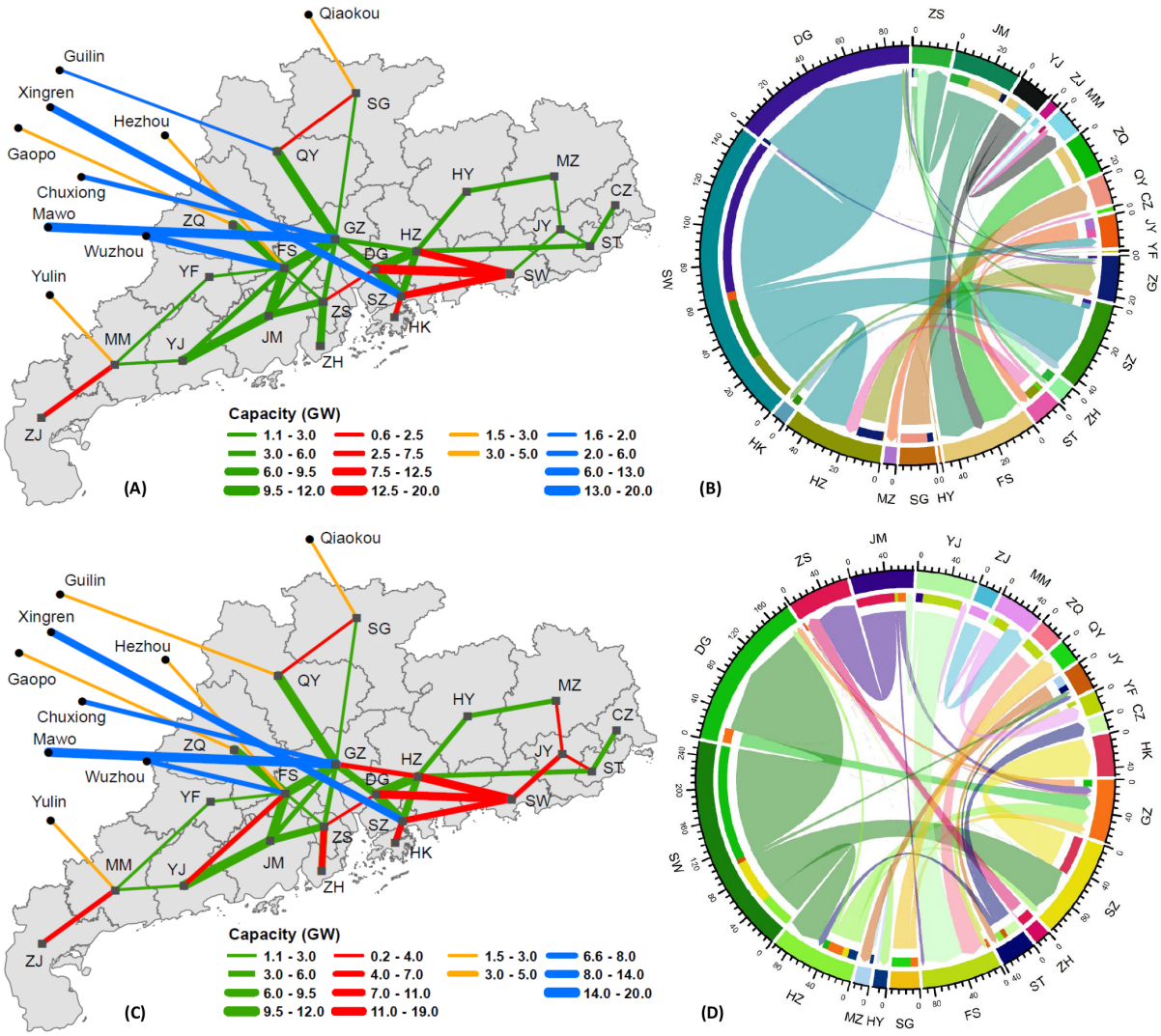

Figure S14 Optimal transmission networks (GW) and annual power flows (TWh) of GHM power system in 2050: (A-B) CDM85 and (C-D) CDM100. (A and C) The yellow and green lines denote existing transmission lines for electricity import and inter-city power transmission, respectively. The blue lines indicate reinforced transmission lines for importing electricity, while the red lines represent reinforced transmission lines for power transmission between cities. (B and D) The node sections denote the total exchanged power. The chord inside the circle indicates the transmitted power, the color denotes destination on node section, and the arrow represents power flow direction between cites.

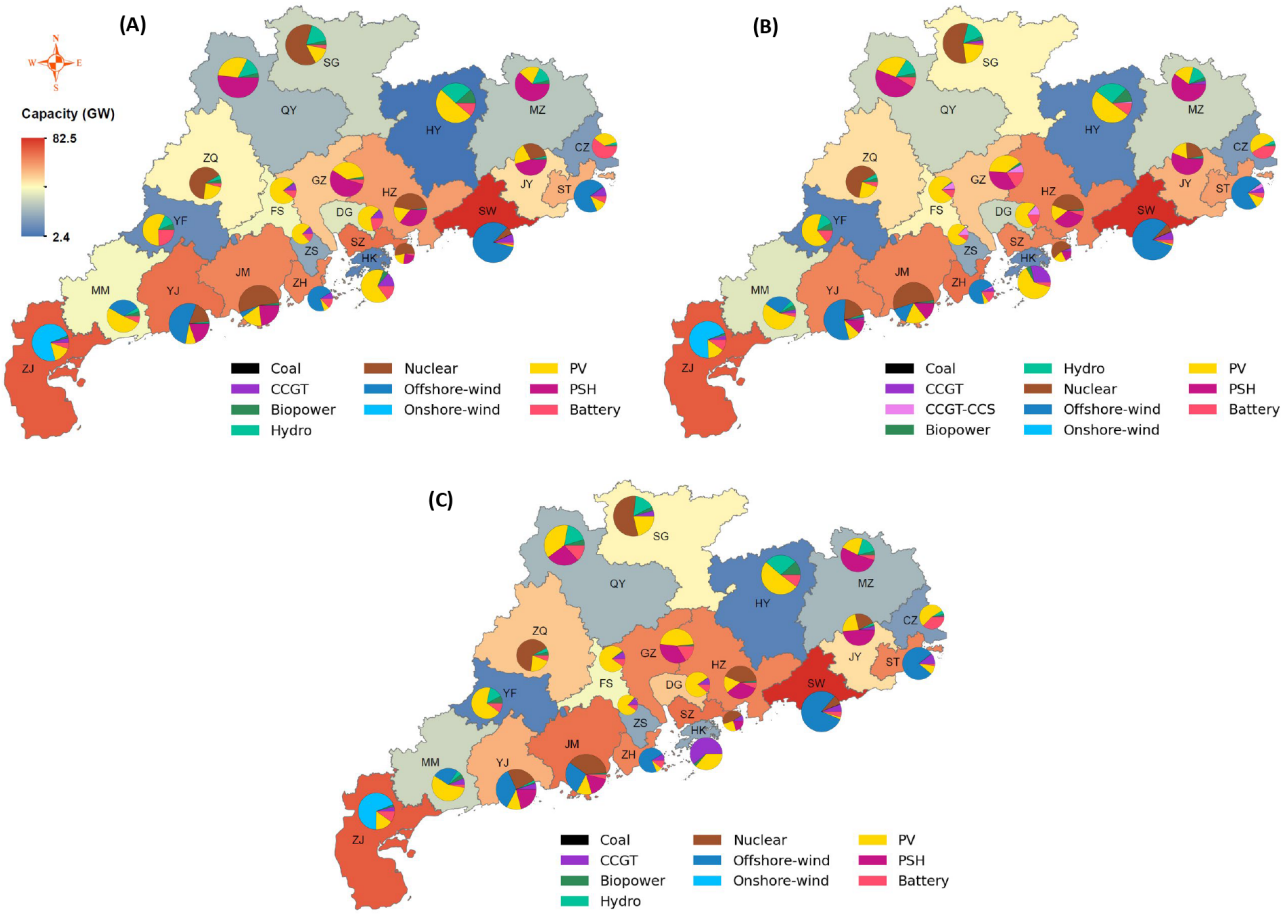

Figure S15 Geographical distribution of generation and storage capacities for GHM power system in 2050: (A) CN35, (B) CN40, and (C) CN45. The color of a city on the map indicates its total installed capacity, whose value can be referred to its color bar. The arc section in the pie chart represents the installed capacity of an energy technology in a city.

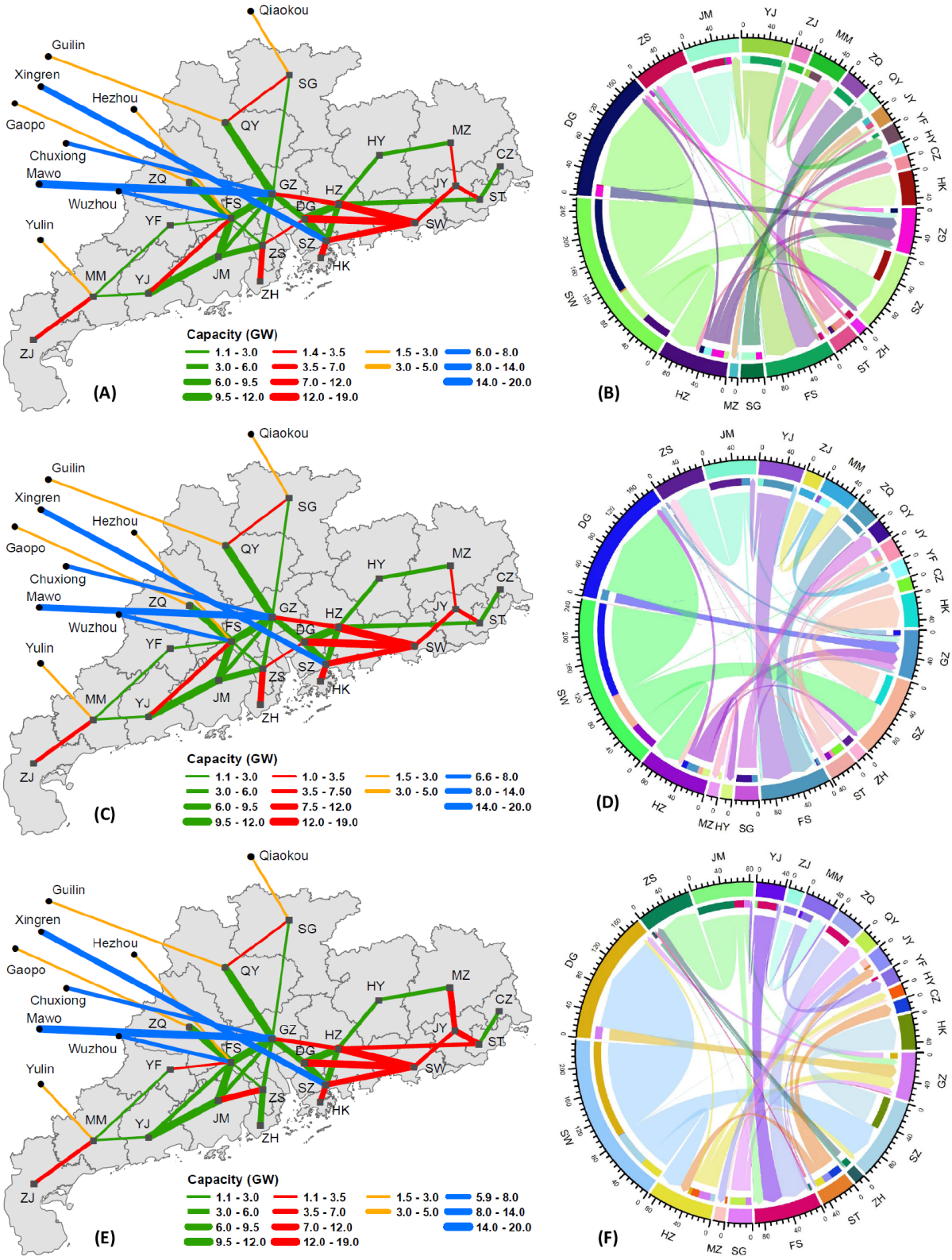

Figure S16 Optimal transmission networks (GW) and annual power flows (TWh) of GHM power system in 2050: (A-B) CN35, (C-D) CN40, and (E-F) CN45. (A, C and E) The yellow and green lines denote existing transmission lines for electricity import and inter-city power transmission, respectively. The blue lines indicate reinforced transmission lines for importing electricity, while the red lines represent reinforced transmission lines for power transmission between cities. (B, D, and F) The node sections denote the total exchanged power. The chord inside the circle indicates the transmitted power, the color denotes destination on node section, and the arrow represents power flow direction between cites.

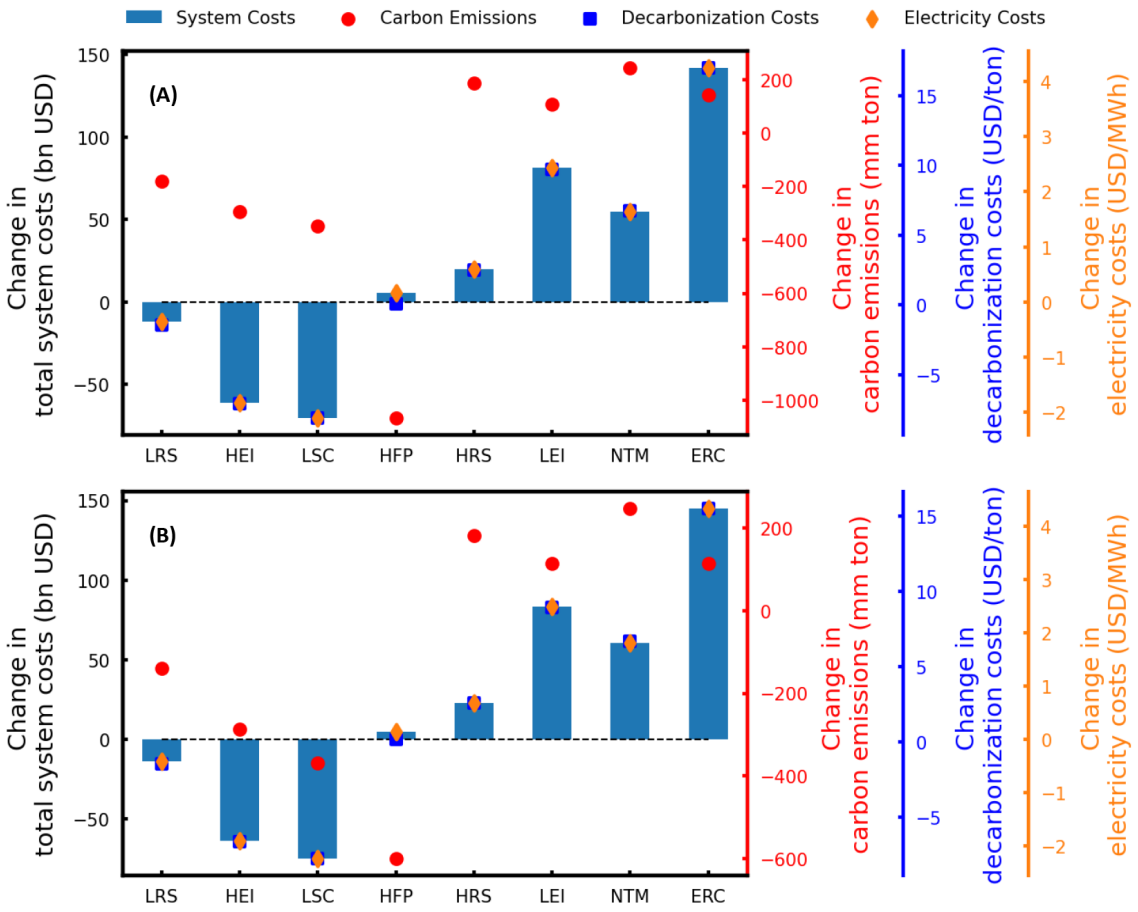

Figure S17 System costs, carbon emissions, decarbonization costs and electricity costs in sensitivity analysis under CDM70 (A) and CDM85 (B). The changes in (A) and (B) are relative to CDM70 and CDM85 respectively. CDM70 (CDM85) has a total system cost of 619.1 (628.3) billion USD, carbon emissions of 5.26 (4.29) billion ton, average decarbonization cost of 4.79 (5.27) USD/ton, and average electricity cost of 18.53 (18.80) USD/MWh.

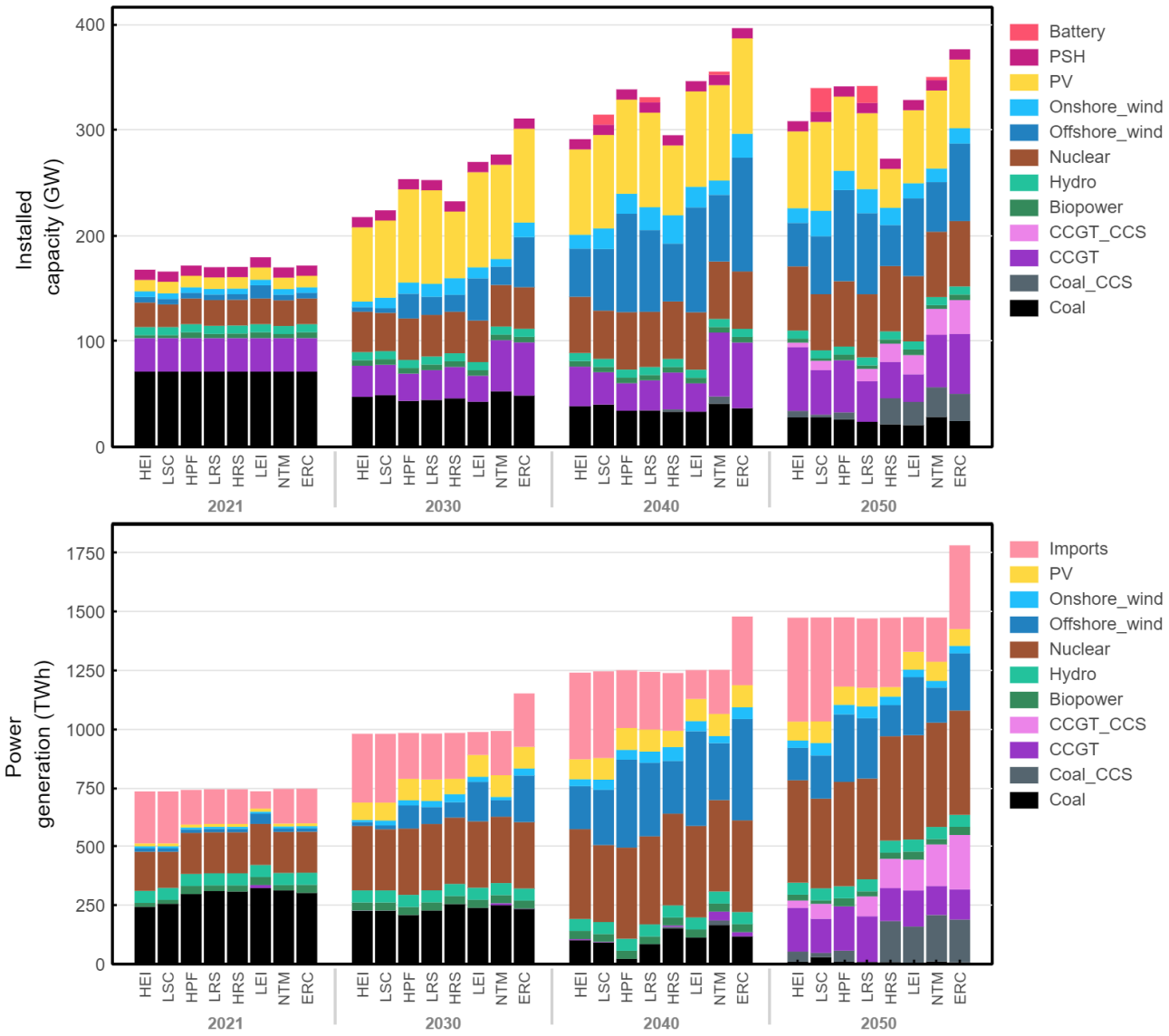

Figure S18 Optimal capacity and generation mix in sensitivity analysis under CDM70 scenario.

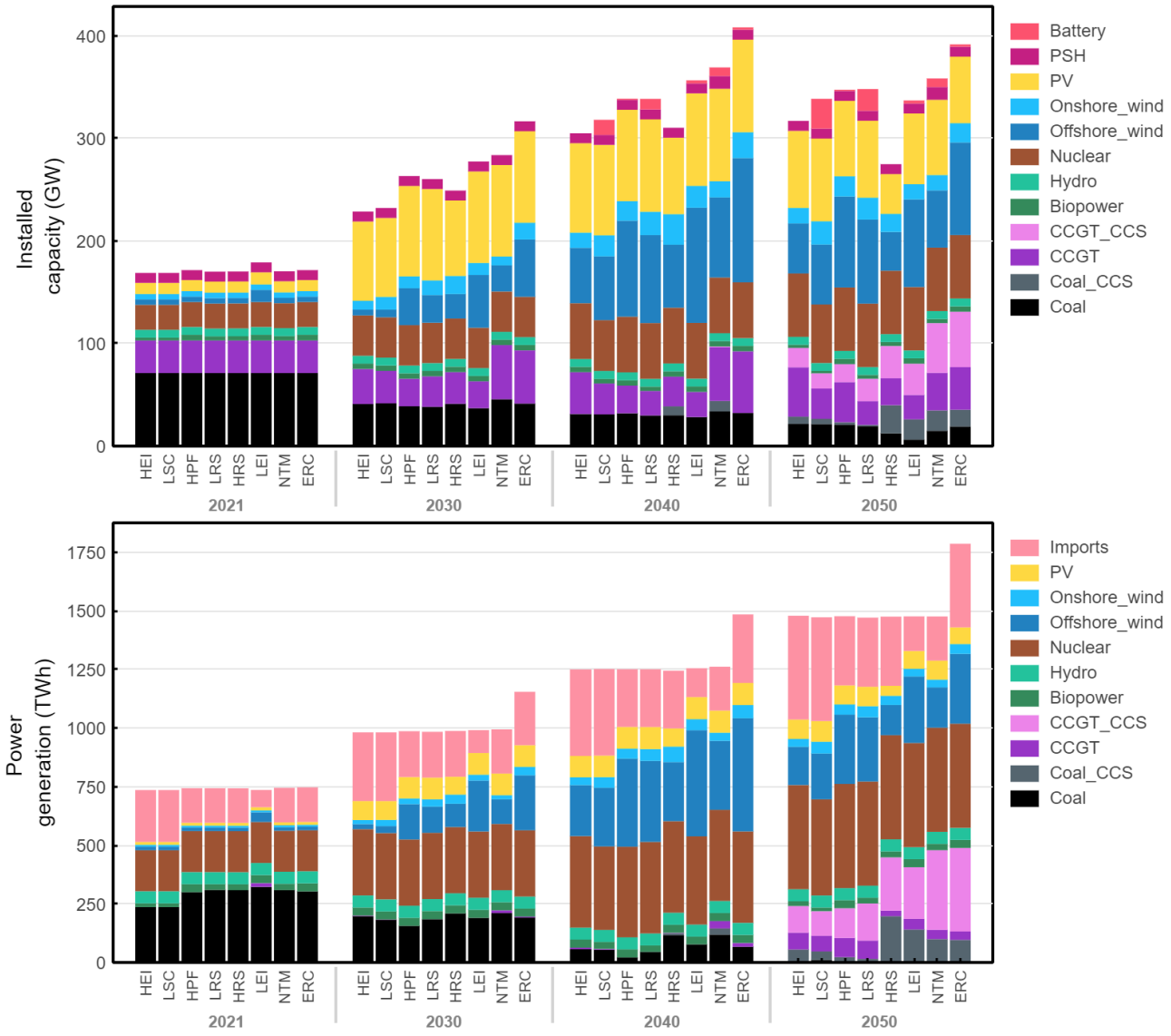

Figure S19 Optimal capacity and generation mix in sensitivity analysis under CDM85 scenario.

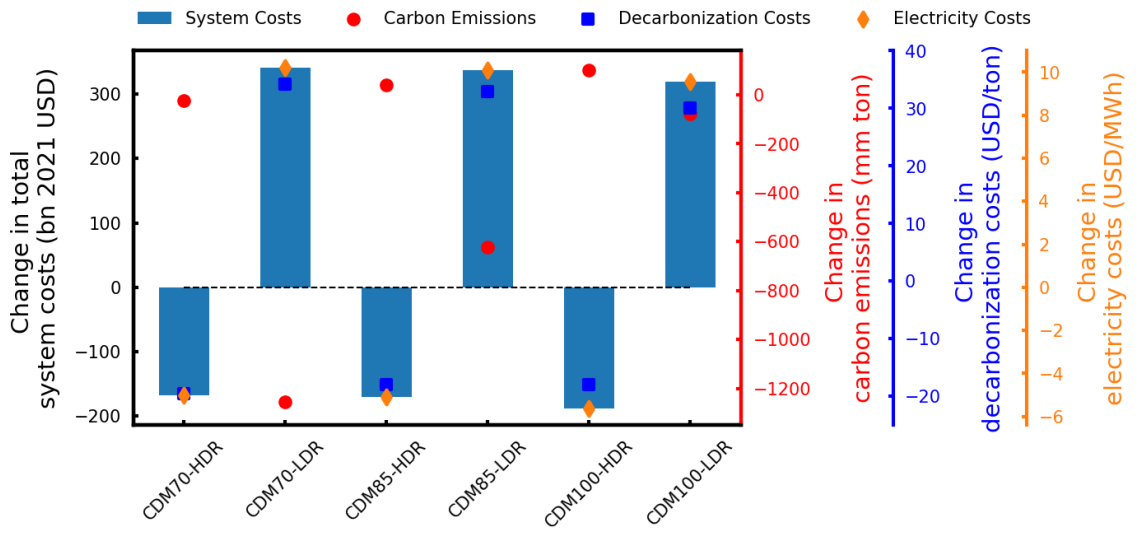

Figure S20 System costs, carbon emissions, decarbonization costs and electricity costs in low (LDR = 3%) and high (HDR = 8%) discount rate cases under CDM70, CDM85, and CDM100 scenarios. The changes are relative to CDM70, CDM85, and CDM100, respectively. CDM70 (CDM85, CDM100) has a total system cost of 619.1 (628.3, 653.1) billion USD, carbon emissions of 5.26 (4.29, 3.26) billion ton, average decarbonization cost of 4.79 (5.27, 7.11) USD/ton, and average electricity cost of 18.53 (18.80, 19.55) USD/MWh.

From Figure S20, we can see that discount rate has a great impact on system decarbonization. A high (low) discount rate indicates low (high) present day values of future costs, and thus can remarkably reduce (increase) total system costs in each scenario. Moreover, a high discount rate (HDR) can lower total system costs by around 175 billion USD under CDM70, CDM85, and CDM100 scenarios, while a low discount rate (LDR) can raise total system costs by around 332 billion USD in these three scenarios. This incurs similar changes in their average decarbonization costs and average electricity costs. However, changes in carbon emissions between HDR and LDR are of difference under CDM70, CDM85, and CDM100. HDR leads to a mild change in carbon emissions across CDM70, CDM85, and CDM100, while LDR results in a radical change in their carbon emissions, varying from -1.26 billion ton in CDM70 to 100.7 million ton in CDM100. This is because LDR renders fossil-based generation more expensive when discounting back to present day value and thus decrease its installation and generation during given planning horizon, as shown especially in 2040 in Figure S21.

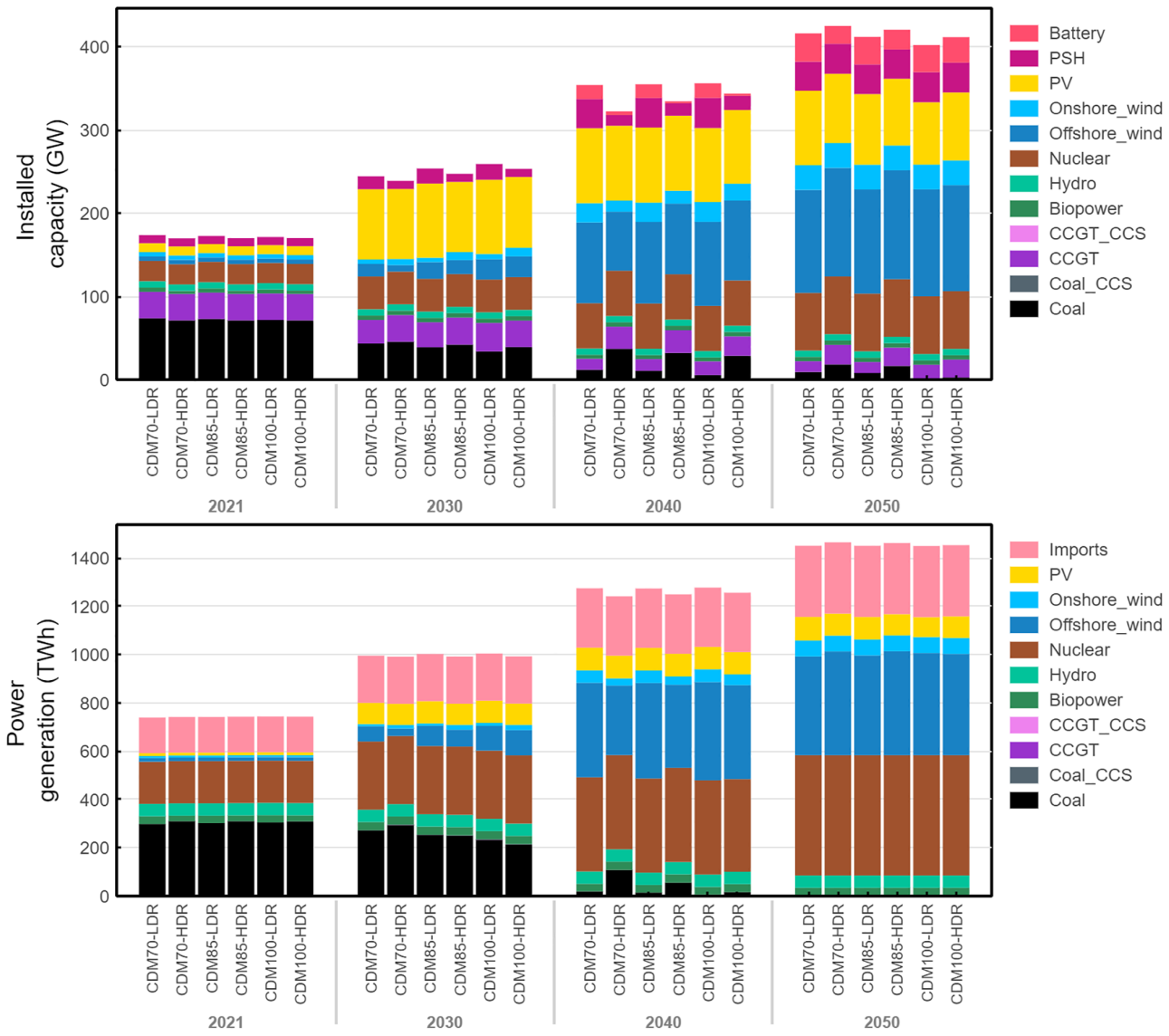

Figure S21 Optimal capacity and generation mix for low (LDR = 3%) and high (HDR = 8%) discount rates under CDM70, CDM85, and CDM100 scenarios.

Supplementary references

1. Global Energy Monitor. Global Coal Plant Tracker; 2022. https://globalenergymonitor.org/projects/global-coal-plant-tracker/.
2. Guangdong Provincial Development and Reform Commission. Energy Bureau of Guangdong Province; 2022.
3. Energy Bureau of Guangdong Province. The 14th Five-Year Plan of Guangdong Province on Energy Development; 2020.
4. Energy Bureau of Guangdong Province. The solar photovoltaic generation development plan of Guangdong Province: 2014-2020; 2014.
5. Energy Bureau of Guangdong Province. The onshare wind generation development plan of Guangdong Province: 2016-2030; 2016.
6. Energy Bureau of Guangdong Province. The offshare wind generation development plan of Guangdong Province: 2017-2030; 2017.
7. Gelaro R, McCarty W, Suarez MJ, Todling R, Molod A, Takacs L, et al. The Modern-Era Retrospective Analysis for Research and Applications, Version 2 (MERRA-2). Journal of Climate. 2017;30(14):5419–5454.
8. Statistics Bureau of Guangdong Province. Guangdong Statistical Yearbook on Agcriculture; 2019.
9. Small-scale hydro generation in Guangdong province. Beijixing Hydro-Generation; 2020.
10. Yu S. Analysis of biomass generation market scale and structure in China; 2020.
11. Gu L. Waste incineartion market in Guandong province; 2022.
12. Power Scheduling and Control Center, China Southern Power Grid Corporation. China Southern Power Grid Opeartion Manners; 2015.
13. Gu H. Research on transmission pricing for West-to-East Power Transmission. South China University of Technology. Master thesis; 2014.
14. Brown PR, Botterud A. The value of inter-regional coordination and transmission in decarbonizing the US electricity system. Joule. 2021;5(1):115–134.
15. Chen X, Liu Y, Wang Q, Lv J, Wen J, Chen X, et al. Pathway toward carbon-neutral electrical systems in China by mid-century with negative CO2 abatement costs informed by high-resolution modeling. Joule. 2021;5(10):2715–2741.
16. Soummane S, Ghersi F. Projecting Saudi sectoral electricity demand in 2030 using a computable general equilibrium model. Energy Strategy Reviews. 2022;39:100787.
17. Wang Y, Wang J, Zhao G, Dong Y. Application of residual modification approach in seasonal ARIMA for electricity demand forecasting: A case study of China. Energy Policy. 2012;48:284–294.

18. Statistics Bureau of Guangdong Province. Guangdong Statistical Yearbook; 2019.

19. Census and Statistics Department. The Government of Hong Kong Special Adminstrative Region; 2021. https://www.censtatd.gov.hk/en/scode90.html.

20. Macau Statistical Yearbook. The Government of Macau Special Adminstrative Region; 2021. https://www.dsec.gov.mo/en-US/Home/Publication/YearbookOfStatistics.

21. MathWorks. Econometrics Toolbox; 2022. https://ww2.mathworks.cn/products/econometrics.html.

22. Li M, Virguez E, Shan R, Tian J, Gao S, Patino-Echeverri D. High-resolution data shows China's wind and solar energy resources are enough to support a 2050 decarbonized electricity system. Applied Energy. 2022;306:117996.

23. Chinese Academy of Sciences. 2018 Land Utilization in China, Remote Sensing Data. Resource and Environment Science and Data Center, Chinese Academy of Sciences; 2019. https://www.resdc.cn/data.aspx?DATAID=264.

24. Chinese Academy of Sciences. DEM 90m Data by Province. Resource and Environment Science and Data Center, Chinese Academy of Sciences; 2018. https://www.resdc.cn/data.aspx?DATAID=284.

25. Chinese Academy of Sciences. Landform Types Distribution in China, 1 Million Resolution. Resource and Environment Science and Data Center, Chinese Academy of Sciences; 2010. https://www.resdc.cn/data.aspx?DATAID=124.

26. Trondle T, Lilliestam J, Marelli S, Pfenninger S. Trade-offs between geographic scale, cost, and infrastructure requirements for fully renewable electricity in Europe. Joule. 2020;4(9):1929–1948.

27. Global Wind Atlas; 2022. https://globalwindatlas.info.

28. General Bathymetric Chart of the Oceans. Gridded bathymetry data; 2020. https://www.gebco.net/data_and_products/gridded_bathymetry_data/.

29. Zeyringer M, Price J, Fais B, Li PH, Sharp E. Designing low-carbon power systems for Great Britain in 2050 that are robust to the spatiotemporal and inter-annual variability of weather. Nature Energy. 2018;3(5):395–403.

30. Feng F, Wang K. Does the modern-era retrospective analysis for research and applications-2 aerosol reanalysis introduce an improvement in the simulation of surface solar radiation over China? International Journal of Climatology. 2019;39(3):1305–1318.

31. Dobos AP. PVWatts version 5 manual. National Renewable Energy Lab.(NREL), Golden, CO (United States); 2014.

32. Bi Y, Gao C, Wang Y, Li B. Estimation of straw resources in China. Transaction of the Chinese Society of Agcricultural Engineering. 2009;25(12):211–217.

33. Fu T, Bao W, Xie G. Methods for assessing resources of forestry residues. Chinese Journal of

Biotechnology. 2018;34(9):1500–1509.

34. Wang F, Li H. Resource utilization and prospect for the greening waste. China Development; 2014.

35. International Renewable Energy Agency. Renewable generation power costs in 2020; 2021.

36. Cole WJ, Greer D, Denholm P, Frazier AW, Machen S, Mai T, et al. Quantifying the challenge of reaching a 100% renewable energy power system for the United States. Joule. 2021;5(7):1732–1748.

37. National Renewable Enegy Laboratory. Annual Technology Baseline; 2022. https://atb.nrel.gov/electricity/2021/data.

38. Zhang S, Chen W. Assessing the energy transition in China towards carbon neutrality with a probabilistic framework. Nature Communications. 2022;13(1):87.

39. Cole W, Frazier AW, Augustine C. Cost projections for utility-scale battery storage: 2021 update. Golden, CO: National Renewable Energy Laboratory; 2021.

40. Coal price index for coal-fired generation in China; 2019. http://www.ccoalnews.com/201905/20/c106271.html.

41. Benchmark prices of gate stations for non-residential natural gas in China; 2015. https://www.ndrc.gov.cn/fzggw/jgsj/jgs/sjdt/201511/t20151118_1109917.html?code=&state=123.

42. Ren C, Han Q. Research on the elastic space of transmission price of west-to-east power transmission project. Souther Energy Construction. 2021;8(1):122–127.

43. Tao Y, Yan M. Hydropower price is going to rise and new energy opens up new growth opportunities. China Galaxy Securities; 2022.

44. National Energy Adminstration. Manual of Renewable Energy Data; 2015. https://www.docin.com/p-1445847621.html.

45. Grid Project Construction Cost Analysis in the 11th Five-year Period. Electric Power Planning & Engineering Institute; 2011.

46. China Electricity Council. China Power Industry Annual Development Report. China Building Materials Press, Beijing; 2020.

47. Zhuo Z, Du E, Zhang N, Nielsen CP, Lu X, Xiao J, et al. Cost increase in the electricity supply to achieve carbon neutrality in China. Nature Communications. 2022;13(1):3172.

48. U.S. Energy Information Administration, Annual Energy Outlook 2015; 2015.

49. Yang F. An analysis of macroeconomic situation and electricity market supply-demand status in Guangdong province. Smart Research Consultance; 2021.

50. China Electricity Council. China Power statistics Year Book; 2021. https://cec.org.cn/detail/index.html?3-301580.